Electronic Supplementary Material (ESI) for Organic & Biomolecular Chemistry.

Supporting Information

One-Step Synthesis of Indolizino[3,4,5-*ab*]isoindoles by Manganese(I)-Catalyzed C–H Activation: Structural Studies and Photophysical Properties

Sara Cembellín,*[a,b] Iván Maisuls,[c] Constantin G. Daniliuc,[a] Helena Osthues,[d] Nikos L. Doltsinis,[d] Cristian A. Strassert[c] and Frank Glorius[a]

[a] Organisch-Chemisches Institut, Westfälische Wilhelms-Universität Münster, Corrensstraße 40, 48149 Münster, Germany.

[b] Organic Chemistry Department, Universidad Complutense de Madrid, 28040 Madrid, Spain.

[c] Institute for Inorganic and Analytical Chemistry, Center for Nanotechnology, Center for Soft Nanoscience, Westfälische Wilhelms-Universität Münster, Heisenbergstraße 11, 48149 Münster, Germany.

[d] Institut für Festkörpertheorie, Westfälische Wilhelms-Universität Münster, Wilhelm-Klemm-Straße 10, 48149 Münster, Germany.

scembellin@ucm.es

Supporting Information

Table of Contents

1. General Information

Unless otherwise noted, all reactions were carried out under an atmosphere of argon in oven-dried glassware cooled down under vacuum. Reaction temperatures are reported as the temperature of the heat transfer medium surrounding the vessel unless otherwise stated.

The following solvents were dried by distillation over the drying agents indicated in parentheses: THF (Na/benzophenone), toluene (CaH_2), Et_2O (Na/benzophenone), CH_2Cl_2 (CaH_2). Additional anhydrous solvents (≤50 ppm water) were purchased from Acros Organics, Sigma-Aldrich, or Carl Roth and stored over molecular sieves under an argon atmosphere.

Commercially available chemicals were obtained from Acros Organics, Aldrich Chemical Co., Alfa Aesar, ABCR, TCI Europe, Combi-Blocks and Fluorochem, and used as received unless otherwise stated.

Analytical thin layer chromatography (TLC) was performed on silica gel 60 F254 aluminum plates (Merck) and they were visualized by exposure to short wave ultraviolet light (254 nm, 366 nm) and/or by staining. For staining the TLC plates were dipped into a solution of $KMnO_4$ (1 g $KMnO_4$, 6 g K_2CO_3 and 0.1 g KOH in 100 mL H_2O) and developed with a heat gun if necessary. Flash chromatography was performed on Merck silica gel (40-63 mesh) by standard techniques using appropriate mixtures of *n*-pentane and ethyl acetate with a positive argon overpressure.

^{1}H- and ^{13}C-NMR spectra were recorded at room temperature on a Bruker AV 300 or AV 400, Varian 500 MHz INOVA or Varian Unity plus 600 in solvents as indicated. Chemical shifts (δ) for ^{1}H- and ^{13}C-NMR spectra are given in ppm relative to tetramethylsilane (TMS) using the residual solvent signals as references for ^{1}H and ^{13}C NMR spectra ($(CD_3)_2CO$: δ_H = 2.05 ppm, δ_C = 29.84, 206.26 ppm).[1] Chemical shifts are generally reported with two (^{1}H) or one (all other nuclei) digits after the decimal point. NMR-data are reported as follows: chemical shift (multiplicity [s = singlet, d = doublet, t = triplet, q = quartet, quint = quintet, sept = septet, m = multiplet,

br = broad], coupling constants (*J*, Hz) and integration). All spectra were processed using the MestReNova program.

High resolution mass spectra (HRMS) were recorded on a Bruker Daltonics MicroTof or on a Thermo-Fisher Scientific Orbitrap LTQ XL spectrometer using electron spray ionization (ESI).

GC-MS spectra were recorded on an Agilent Technologies 7890A GC-system with an Agilent 5975C VL MSD or an Agilent 5975 inert Mass Selective Detector (EI) and an HP-5MS column (30 m, 0.32mm, film: 0.25 µm). The major signals are quoted in *m*/*z* with the relative intensity in parentheses.

2. Synthesis of Substrates

2-Phenylpyridine (**1a**) is commercially available while compounds **1b-f** were prepared from 2-bromopyridine and the corresponding boronic acids as reported in the literature.[2] 2-(4-methoxyphenyl)pyridine (**1b**), 2-(4-chlorophenyl)pyridine (**1c**), 2-(4-bromophenyl)pyridine (**1d**), 2-(4-iodophenyl)pyridine (**1e**) and 2-(naphthalen-2-yl)pyridine (**1f**) are known compounds and their spectral data are in agreement with the literature values.[3] 1,3-Enyne **2** was prepared from isobutyryl chloride and bis(trimethylsilyl)- acetylene in two steps without need of purification according to a procedure described in the literature.[4] All the protocols were employed without any optimization of the reaction conditions.

3. Optimization of the Reaction Conditions

General procedure for the optimization of the reaction conditions:

In a 10 mL oven-dried Schlenk tube with a stirring bar, 2-phenylpyridine (**1a**, 0.1 mmol, 14.3 µL), 4-methyl-1-(trimethylsilyl)pent-3-en-1-yn-3-yl trifluoromethane-sulfonate (**2**, 0.15 mmol, 45.1 mg), $MnBr(CO)_5$ (10 mol%, 2.7 mg) and the base were added under air. Then, the reaction vessel was evacuated and filled with argon three times. Afterwards, the respective solvent (0.5 mL) was added under an argon

atmosphere. The tube was sealed and the mixture was stirred (1100r/min) at the appropriate temperature for indicated time. The reaction was allowed to cool to room temperature and the volatiles were removed. Yield was determined by ^{1}H-NMR analysis using 1,2-dibromomethane (7 μL, 0.1 mmol) as the internal standard.

Table S1. Optimization of reaction conditions.

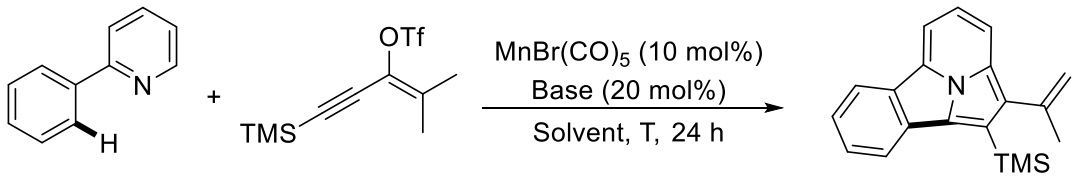

1a **2** **3a**

Entry	Solvent	Base	Additive	T (ºC)	Conversion of 1a (%)	Yield of 3a (%)
1	Et_2O	Cy_2NH	-	90	15	13
2	1,4-dioxane	Cy_2NH	-	90	10	10
3	**DCE**	**Cy_2NH**	**-**	**90**	**17**	**15**
4	DMF	Cy_2NH	-	90	0	n.d.
5	toluene	Cy_2NH	-	90	10	10
6	DME	Cy_2NH	-	90	5	5
7	THF	Cy_2NH	-	90	0	n.d.
8	MeCN	Cy_2NH	-	90	0	n.d.
9	MeOH	Cy_2NH	-	90	0	n.d.
10	DMA	Cy_2NH	-	90	0	n.d.
11	DCM	Cy_2NH	-	90	15	15
12[a]	DCE	Cy_2NH	-	rt	5	5
13	DCE	Cy_2NH	-	135	20	15
14	DCE	NaOAc	-	90	10	10

15	DCE	K_3PO_4	-	90	10	10
16	DCE	$^{i}PrNH_2$	-	90	15	10
17	DCE	DBU	-	90	14	10
18	DCE	DIPEA	-	90	10	10
19	DCE	Cy_2NH	BPh_3	90	15	15
20	DCE	Cy_2NH	H_2O	90	14	10
21	DCE	Cy_2NH	HOAc	90	13	10
22	DCE	Cy_2NH	PPh_3	90	10	8
23	DCE	Cy_2NH	$Cu(OAc)_2 \cdot H_2O$	90	10	10
24	DCE	Cy_2NH	$CuBr_2$	90	15	13
25	DCE	Cy_2NH	DDQ	90	0	0
26[b]	DCE	Cy_2NH	-	90	15	12
27[c]	DCE	Cy_2NH	-	90	17	15
28[d]	DCE	Cy_2NH	-	90	17	14
29[e]	DCE	Cy_2NH	-	rt	0	0

[a] The time of the reaction was 48h. [b] 1 equiv. of **2** was used. [c] 2 equiv. of **2** were used. [d] MW was used instead of heating. [e] Irradiation with 450 nm LED spot of 40 W. DCE = 1,2-Dichloroethane. DMF = *N,N*- Dimethylformamide. DME = 1,2-Dimethoxyethane. THF = Tetrahydrofuran. DMA = *N,N*- Dimethylacetamide. DCM = Dichloromethane. DBU = 1,8-Diazabicyclo[5.4.0]undec-7-ene. DIPEA = *N,N*-Diisopropylethylamine.

4. Procedure and Analytical Data of Compounds 3

*General procedure for the synthesis of indolizino[3,4,5-*ab*]isoindoles:*

In a 10 mL oven-dried Schlenk tube with a stirring bar, **1** (0.2 mmol), 4-methyl-1-(trimethylsilyl)pent-3-en-1-yn-3-yl trifluoromethanesulfonate (**2**, 0.3 mmol, 90.2 mg), $MnBr(CO)_5$ (10 mol%, 5.4 mg) and Cy_2NH (20 mol%, 8μL) were added

under air. Then, the reaction vessel was evacuated and filled with argon three times. Afterwards, DCE (1 mL) was added under an argon atmosphere. The tube was sealed and the mixture was stirred (1100r/min) at 90 ºC for 24h. The reaction was allowed to cool to room temperature, the volatiles were removed and the analytically pure product **3** was obtained by flash chromatography (silica gel; pentane/EtOAc).

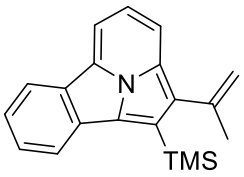

2-(prop-1-en-2-yl)-1-(trimethylsilyl) indolizino [3,4,5-*ab*] isoindole: Following the general procedure, the reaction of 2-phenylpyridine (**1a**) (0.2 mmol, 28.6 µL), 4-methyl-1-(trimethylsilyl)pent-3-en-1-yn-3-yl trifluoromethane sulfonate (**2**) (0.15 mmol, 90.2 mg), $MnBr(CO)_5$ (10 mol%, 5.4 mg) and Cy_2NH (20 mol%, 8 µL) in DCE (1 mL) at 90 ºC for 24h afforded the product **3a** (15%, 9.2 mg) as a yellow solid. **^{1}H NMR (600 MHz, $(CD_3)_2CO$)** δ 8.60 (dt, *J* = 8.0, 0.9 Hz, 1H), 8.34 (d, *J* = 8.2 Hz, 1H), 8.31 (d, *J* = 7.4 Hz, 1H), 8.10 (d, *J* = 8.3 Hz, 1H), 7.81 – 7.70 (m, 2H), 7.54 (ddd, *J* = 8.0, 7.2, 0.9 Hz, 1H), 5.45 (dq, *J* = 2.9, 1.5 Hz, 1H), 5.15 (dd, *J* = 2.6, 0.9 Hz, 1H), 2.43 – 2.27 (m, 3H), 0.59 (s, 9H); **^{13}C NMR (151 MHz, $(CD_3)_2CO$)** δ 141.1, 131.0, 130.0, 128.7, 128.0, 127.7, 127.2, 127.0, 126.2, 122.7, 122.5, 120.1, 119.2, 116.8, 114.5, 108.4, 26.1, 0.5; **HRMS** m/z (ESI) calcd. for $C_{20}H_{21}NSi$ (M^+): 303.1443, found 303.1441.

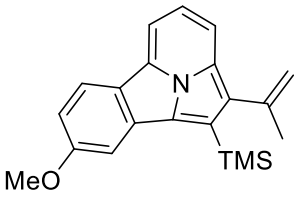

8-methoxy-2-(prop-1-en-2-yl)-1-(trimethylsilyl)indolizino [3,4,5-*ab*]isoindole: Following the general procedure, the reaction of 2-(4-methoxyphenyl)pyridine (**1b**) (0.2 mmol, 37.0 mg), 4-methyl-1-(trimethylsilyl)pent-3-en-1-yn-3-yl trifluoromethane sulfonate (**2**) (0.3 mmol, 90.2 mg), $MnBr(CO)_5$ (10 mol%, 5.4 mg) and Cy_2NH (20 mol%, 8µL) in DCE (1 mL) at 90 ºC for 24h afforded the product **3b** (13%, 9.0 mg) as a yellow solid. **^{1}H NMR (300 MHz, $(CD_3)_2CO$)** δ 8.45 (d, *J* = 8.8 Hz, 1H), 8.14 (d, *J* = 7.3 Hz, 1H), 7.98 (d, *J* = 8.3 Hz, 1H), 7.74 – 7.63 (m, 2H), 7.15 (dd, *J* = 8.8, 2.3 Hz, 1H), 5.42 (dd, *J* = 2.6, 1.4 Hz, 1H), 5.12 (dd, *J* = 2.5, 0.8 Hz, 1H), 3.99 (s, 3H), 2.32 (bs, 3H), 0.58 (s, 9H); **^{13}C NMR (126 MHz, $(CD_3)_2CO$)** δ 161.4, 142.2, 132.7, 131.9, 130.7, 128.5, 128.2, 124.8, 123.7, 123.0, 120.6, 117.9, 114.3, 113.1, 108.2,

103.6, 56.1, 27.2, 1.6; **HRMS** m/z (ESI) calcd. for $C_{21}H_{23}NOSi$ (M^+): 333.1549, found 333.1552.

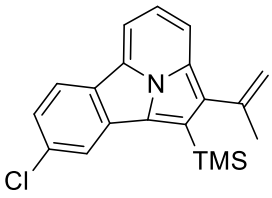

8-chloro-2-(prop-1-en-2-yl)-1-(trimethylsilyl)indolizino[3,4,5-*ab*]isoindole: Following the general procedure, the reaction of 2-(4-chlorophenyl)pyridine (**1b**) (0.2 mmol, 38.0 mg), 4-methyl-1-(trimethylsilyl)pent-3-en-1-yn-3-yl trifluoromethane sulfonate (**2**) (0.3 mmol, 90.2 mg), $MnBr(CO)_5$ (10 mol%, 5.4 mg) and Cy_2NH (20 mol%, 8µL) in DCE (1 mL) at 90 ºC for 24h afforded the product **3c** (20%, 13.4 mg) as a yellow solid. **^{1}H NMR (300 MHz, $(CD_3)_2CO$)** δ 8.63 (d, *J* = 8.5 Hz, 1H), 8.38 (d, *J* = 7.3 Hz, 1H), 8.28 (d, *J* = 1.4 Hz, 1H), 8.15 (d, *J* = 8.3 Hz, 1H), 7.81 (dd, *J* = 8.3, 7.4 Hz, 1H), 7.55 (dd, *J* = 8.5, 1.9 Hz, 1H), 5.48 (dd, *J* = 2.5, 1.5 Hz, 1H), 5.17 (dd, *J* = 2.5, 0.9 Hz, 1H), 2.40 – 2.33 (m, 3H), 0.60 (s, 9H); **^{13}C NMR (75 MHz, $(CD_3)_2CO$)** δ 140.3, 132.8, 131.5, 130.1, 127.1, 126.3, 126.1, 124.6, 123.7, 123.1, 122.0, 119.5, 118.8, 116.7, 114.3, 108.7, 25.5, 0.0; **HRMS** m/z (ESI) calcd. for $C_{20}H_{20}ClNSi$ (M^+): 337.1054, found 337.1050.

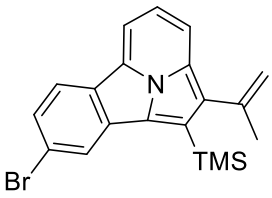

8-bromo-2-(prop-1-en-2-yl)-1-(trimethylsilyl)indolizino[3,4,5-*ab*]isoindole: Following the general procedure, the reaction of 2-(4-bromophenyl)pyridine (**1d**) (0.2 mmol, 46.8 mg), 4-methyl-1-(trimethylsilyl)pent-3-en-1-yn-3-yl trifluoromethane sulfonate (**2**) (0.3 mmol, 90.2 mg), $MnBr(CO)_5$ (10 mol%, 5.4 mg) and Cy_2NH (20 mol%, 8µL) in DCE (1 mL) at 90 ºC for 24h afforded the product **3d** (17%, 12.8 mg) as a yellow solid. **^{1}H NMR (700 MHz, $(CD_3)_2CO$)** δ 8.58 (d, *J* = 8.6 Hz, 1H), 8.45 (dd, *J* = 8.3, 1.6 Hz, 1H), 8.40 (d, *J* = 7.2 Hz, 1H), 8.17 (d, *J* = 8.2 Hz, 1H), 7.82 (dd, *J* = 8.2, 7.3 Hz, 1H), 7.68 (dd, *J* = 8.4, 1.7 Hz, 1H), 5.48 (dd, *J* = 2.5, 1.4 Hz, 1H), 5.17 (dd, *J* = 2.4, 0.8 Hz, 1H), 2.37-2.35 (m, 3H), 0.61 (s, 9H); **^{13}C NMR (176 MHz, $(CD_3)_2CO$)** δ 141.8, 133.0, 131.8, 131.5, 128.5, 128.0, 127.6, 126.2, 125.7, 125.5, 124.6, 123.4, 121.0, 118.2, 115.9, 110.3, 27.0, 1.5; **HRMS** m/z (ESI) calcd. for $C_{20}H_{20}BrNSi$ (M^+): 381.0548, found 381.0544.

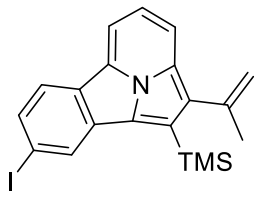

8-iodo-2-(prop-1-en-2-yl)-1-(trimethylsilyl)indolizino[3,4,5-*ab*]isoindole: Following the general procedure, the reaction of 2-(4-iodophenyl)pyridine (**1e**) (0.2 mmol, 56.2 mg), 4-methyl-1-(trimethylsilyl)pent-3-en-1-yn-3-yl trifluoromethane sulfonate (**2**) (0.3 mmol, 90.2 mg), $MnBr(CO)_5$ (10 mol%, 5.4 mg) and Cy_2NH (20 mol%, 8µL) in DCE (1 mL) at 90 ºC for 24h afforded the product **3e** (13%, 11.2 mg) as a yellow solid. **^{1}H NMR (700 MHz, $(CD_3)_2CO$)** δ 8.70 (dd, *J* = 10,3, 1.2 Hz, 1H), 8.45 (d, *J* = 8.3 Hz, 1H), 8.40 (d, *J* = 7.2 Hz, 1H), 8.17 (d, *J* = 8.2 Hz, 1H), 7.87 (dd, *J* = 8.3, 1.5 Hz, 1H), 7.82 (d, *J* = 8.3 Hz, 1H), 5.48 (dd, *J* = 2.5, 1.4 Hz, 1H), 5.17 (dd, *J* = 2.4, 0.8 Hz, 1H), 2.36 (s, 3H), 0.60 (s, 9H); **^{13}C NMR (176 MHz, $(CD_3)_2CO$)** δ 141.8, 137.9, 133.0, 132.2, 131.8, 131.3, 129.8, 128.4, 125.5, 124.4, 120.9, 119.5, 118.2, 116.1, 110.3, 94.3, 27.0, 1.5; **HRMS** m/z (ESI) calcd. for $C_{20}H_{20}INSi$ (M^+): 429.0410, found 429.0402.

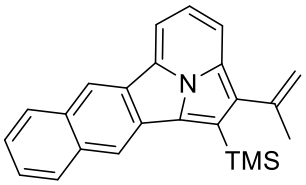

2-(prop-1-en-2-yl)-1-(trimethylsilyl)benzo[f]indolizino[3,4,5-*ab*]isoindole: Following the general procedure, the reaction of 2-(naphthalen-2-yl)pyridine (**1f**) (0.2 mmol, 41.1 mg), 4-methyl-1-(trimethylsilyl)pent-3-en-1-yn-3-yl trifluoro methane sulfonate (**2**) (0.3 mmol, 90.2 mg), $MnBr(CO)_5$ (10 mol%, 5.4 mg) and Cy_2NH (20 mol%, 8µL) in DCE (1 mL) at 90 ºC for 24h afforded the product **3f** (11%, 7.6 mg) as a yellow solid. **^{1}H NMR (300 MHz, $(CD_3)_2CO$)** δ 9.20 – 9.14 (m, 1H), 8.80 – 8.75 (m, 1H), 8.29 – 8.24 (m, 1H), 8.23 (d, *J* = 7.6 Hz, 2H), 8.03 (d, *J* = 8.4 Hz, 1H), 7.67 – 7.62 (m, 1H), 7.57 (d, *J* = 7.8 Hz, 2H), 5.46 (dd, *J* = 2.5, 1.5 Hz, 1H), 5.17 – 5.15 (m, 1H), 2.36 (s, 3H), 0.65 (s, 9H); **^{13}C NMR (176 MHz, $(CD_3)_2CO$)** δ 142.1, 135.3, 134.4, 130.6, 129.6, 129.4, 127.3, 127.1, 126.8, 125.6, 125.4, 122.8, 120.5, 119.0, 118.4, 118.1, 117.7, 117.6, 116.2, 107.4, 26.99, 1.4; **HRMS** m/z (ESI) calcd. for $C_{24}H_{23}NSi$ (M^+): 353.1600, found 353.1611.

Compounds detected but not characterized:

The following compounds were detected by TLC and GC-MS but not fully characterized due to the low conversion of the substrates:

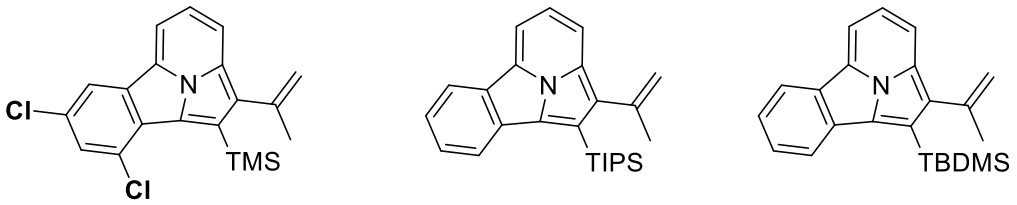

Figure S1. Indolizino[3,4,5-*ab*]isoindoles obtained through the described protocol but not characterized.

5. Mechanistic Studies

5.1. Stoichiometric Reaction

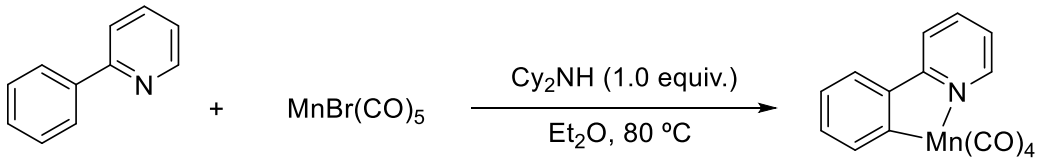

1a (1.0 equiv.) (1.0 equiv.) **4**

Compound **4** was prepared following a procedure previously reported in the literature.[2] In a 10 mL oven-dried Schlenk tube with a stirring bar, $MnBr(CO)_5$ (0.5 mmol, 137.5 mg) was added under a nitrogen atmosphere. Ethyl ether (2.0 ml), 2-phenylpyridine (**1a**, 0.5 mmol, 77.5 mg) and Cy_2NH (0.5 mmol, 90.5 mg) were then injected into the reaction tube. The reaction mixture was stirred at 80 ºC for 6 h. The reaction was allowed to cool to room temperature, the mixture was diluted with ethyl acetate (20 ml) and filtered through a short pad of silica gel. The volatiles were removed and the analytically pure product **4** was obtained by flash chromatography (silica gel; pentane/EtOAc).

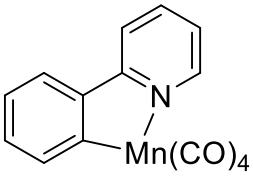

Following the procedure, the reaction afforded the product **4** (84%, 134.9 mg). **^{1}H NMR (300 MHz, $CDCl_3$)** δ 8.75 (d, *J* = 5.0 Hz, 1H), 8.03 – 8.01 (m, 1H), 7.91 (d, *J* = 8.0 Hz, 1H), 7.83 – 7.79 (m, 2H), 7.29 – 7.20 (m, 2H), 7.17 – 7.15 (m, 1H). Spectral data is in accordance with the literature.[2]

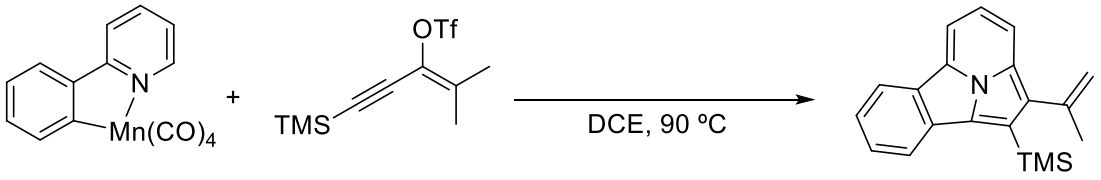

4 (1.0 equiv.) **2** (1.5 equiv.) **3a**

In a 10 mL oven-dried Schlenk tube with a stirring bar, compound **4** (0.42 mmol, 134 mg) and 4-methyl-1-(trimethylsilyl)pent-3-en-1-yn-3-yl trifluoromethanesulfonate (**2**, 0.63 mmol, 189 mg) were added under air. Then, the reaction vessel was evacuated and filled with argon three times. Afterwards, DCE (2.1 mL) was added under an argon atmosphere. The tube was sealed and the mixture was stirred (1100r/min) at 90 ºC for 24h. The reaction was allowed to cool to room temperature, the volatiles were removed and the analytically pure product **3a** was obtained by flash chromatography (silica gel; pentane/EtOAc) in 20% yield (25.1 mg).

5.2. Screening of Different Catalysts

Following the general procedure for the synthesis of indolizino[3,4,5-*ab*]isoindoles, in a 10 mL oven-dried Schlenk tube with a stirring bar, 2-phenylpyridine (**1a**, 0.1 mmol, 14.3 µL), 4-methyl-1-(trimethylsilyl)pent-3-en-1-yn-3-yl trifluoromethanesulfonate (**2**, 0.15 mmol, 45.1 mg) and Cy_2NH (20 mol%, 4µL) were added under air. Then, the reaction vessel was evacuated and filled with argon three times. Afterwards, the corresponding catalyst (10 mol%) and DCE (0.5 mL) were added under an argon atmosphere. The tube was sealed and the mixture was stirred (1100r/min) at 90 ºC for 24h. The reaction was allowed to cool to room temperature and the volatiles were removed. Yield was determined by ^{1}H-NMR analysis using 1,2-dibromomethane (7 µL, 0.1 mmol) as the internal standard.

Table S2. Screening of different catalysts.

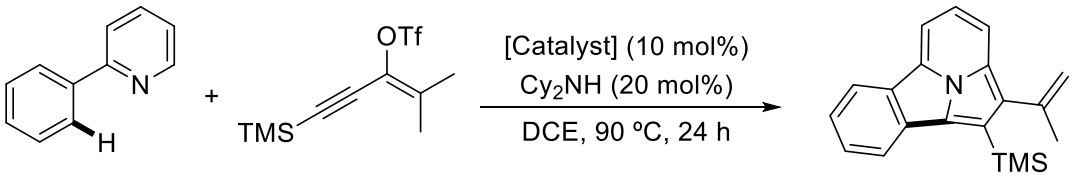

1a **2** **3a**

Entry	Catalyst	Yield of 3a (%)
1	$Pd(OAc)_2$	0
2	$Cp^*Co(CO)I_2$	0
3	$[Cp^*RhCl_2]_2$	0
4	$[Ru(p\text{-cymene})Cl_2]_2$	0
5	**$MnBr(CO)_5$**	**15**
6	**$Mn_2(CO)_{10}$**	**15**

5.3. Screening of Different 1,3-Enynes

Following the general procedure for the synthesis of indolizino[3,4,5-*ab*]isoindoles, in a 10 mL oven-dried Schlenk tube with a stirring bar, 2-phenylpyridine (**1a**, 0.1 mmol, 14.3 μL), 1,3-enyne trifluoromethanesulfonate (**2**, 0.15 mmol), $MnBr(CO)_5$ (10 mol%, 2.7 mg) and Cy_2NH (20 mol%, 4μL) were added under air. Then, the reaction vessel was evacuated and filled with argon three times. Afterwards, DCE (0.5 mL) was added under an argon atmosphere. The tube was sealed and the mixture was stirred (1100r/min) at 90 ºC for 24h. The reaction was allowed to cool to room temperature and the volatiles were removed. Yield was determined by ^{1}H-NMR analysis using 1,2-dibromomethane (7 μL, 0.1 mmol) as the internal standard.

Table S3. Screening of different 1,3-enynes.

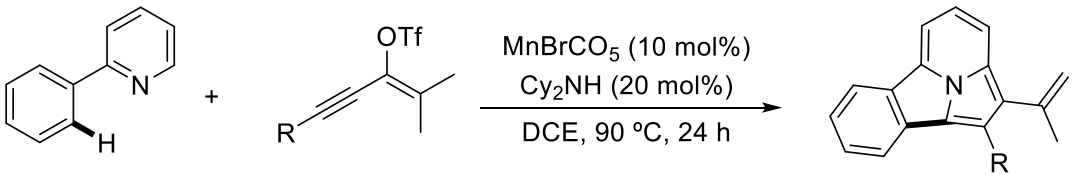

1a **2** **3**

Entry	R	Yield of 3 (%)
1	Me	0
2	Ph	0
3	TIPS	12
4	TBDMS	9

6. X-Ray Diffractometric Analysis

X-Ray diffraction: Data sets for compound **3c** were collected with a Nonius Kappa CCD diffractometer. Programs used: data collection, COLLECT (R. W. W. Hooft, Bruker AXS, **2008**, Delft, The Netherlands); data reduction Denzo-SMN (Z. Otwinowski, W. Minor, *Methods Enzymol.* **1997**, *276*, 307-326); absorption correction, Denzo (Z. Otwinowski, D. Borek, W. Majewski, W. Minor, *Acta Crystallogr*. **2003**, *A59*, 228-234); structure solution *SHELXT-2015* (Sheldrick, G. M. *Acta Cryst.,* **2015**, *A71*, 3-8); structure refinement *SHELXL-2015* (Sheldrick, G. M. *Acta Cryst.,* **2015**, *C71* (1), 3-8) and graphics, *XP* (Version 5.1, Bruker AXS Inc., Madison, Wisconsin, USA, **1998**). *R*-values are given for observed reflections, and wR^2 values are given for all reflections.

Exceptions and special features: For compound **3c** the isopropenyl group was found disordered over two positions. Several restraints (SADI, SAME, ISOR and SIMU) were used in order to improve refinement stability.

X-ray diffractometric crystal structure analysis of 3c: A yellow plate-like specimen of $C_{20}H_{20}ClNSi$, approximate dimensions 0.020 mm x 0.080 mm x 0.100 mm, was used for the X-ray crystallographic analysis. The X-ray intensity data were measured.

The integration of the data using a triclinic unit cell yielded a total of 5254 reflections to a maximum θ angle of 26.37° (0.80 Å resolution), of which 3548 were independent (average redundancy 1.481, completeness = 97.0%, R_{int} = 4.29%, R_{sig} = 4.37%) and 3020 (85.12%) were greater than $2\sigma(F^2)$. The final cell constants of a = 8.4528(3) Å, b

= 10.0726(4) Å, c = 11.6966(6) Å, α = 77.560(4)°, β = 75.781(3)°, γ = 68.597(2)°, volume = 890.01(7) Å^3, are based upon the refinement of the XYZ-centroids of reflections above 20 σ(I). Data were corrected for absorption effects using the multi-scan method (SADABS). The calculated minimum and maximum transmission coefficients (based on crystal size) are 0.9720 and 0.9940.

The structure was solved and refined using the Bruker SHELXTL Software Package, using the space group P -1, with Z = 2 for the formula unit, $C_{20}H_{20}ClNSi$. The final anisotropic full-matrix least-squares refinement on F^2 with 232 variables converged at R1 = 5.23%, for the observed data and wR2 = 13.53% for all data. The goodness-of-fit was 1.068. The largest peak in the final difference electron density synthesis was 0.266 e-/Å^3 and the largest hole was -0.278 e-/Å^3 with an RMS deviation of 0.056 e-/Å^3. On the basis of the final model, the calculated density was 1.261 g/cm^3 and F(000), 356 e-. CCDC Nr.: 2032083.

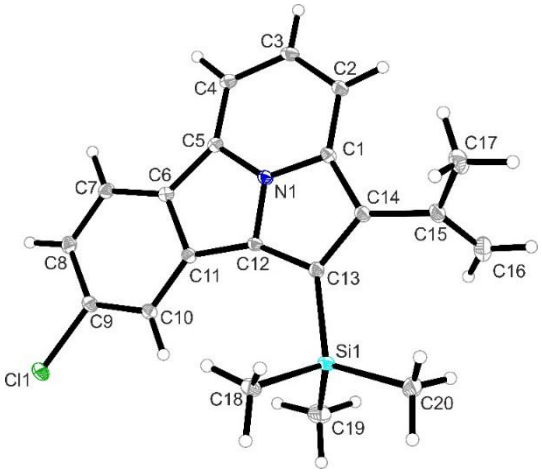

Figure S2. Molecular structure in the crystal of compound **3c** (CCDC 2032083, Thermals ellipsoids are shown with 15% probability).

Table S4. Bond lengths (Å) for compound **3c**.

Cl1-C9	1.748(2)	N1-C12	1.366(3)
N1-C1	1.371(3)	N1-C5	1.371(3)
Si1-C20	1.861(3)	Si1-C18	1.862(3)
Si1-C19	1.864(3)	Si1-C13	1.877(2)
C1-C2	1.404(3)	C1-C14	1.425(3)
C2-C3	1.383(3)	C2-H2	0.95

C3-C4	1.413(3)	C3-H3	0.95
C4-C5	1.372(3)	C4-H4	0.95
C5-C6	1.445(3)	C6-C7	1.398(3)
C6-C11	1.437(3)	C7-C8	1.380(3)
C7-H7	0.95	C8-C9	1.401(4)
C8-H8	0.95	C9-C10	1.379(3)
C10-C11	1.401(3)	C10-H10	0.95
C11-C12	1.445(3)	C12-C13	1.423(3)
C13-C14	1.419(3)	C14-C15	1.483(3)
C15-C16A	1.278(19)	C15-C16	1.295(10)
C15-C17	1.534(9)	C15-C17A	1.553(17)
C16-H16A	0.95	C16-H16B	0.95
C17-H17A	0.98	C17-H17B	0.98
C17-H17C	0.98	C16A-H16C	0.95
C16A-H16D	0.95	C17A-H17D	0.98
C17A-H17E	0.98	C17A-H17F	0.98
C18-H18A	0.98	C18-H18B	0.98
C18-H18C	0.98	C19-H19A	0.98
C19-H19B	0.98	C19-H19C	0.98
C20-H20A	0.98	C20-H20B	0.98
C20-H20C	0.98		

Table S5. Bond angles (º) for compound **3c**.

C12-N1-C1	113.56(19)	C12-N1-C5	116.59(18)
C1-N1-C5	129.78(19)	C20-Si1-C18	106.85(13)
C20-Si1-C19	109.89(14)	C18-Si1-C19	108.99(15)
C20-Si1-C13	107.19(11)	C18-Si1-C13	114.65(11)
C19-Si1-C13	109.18(13)	N1-C1-C2	114.0(2)
N1-C1-C14	104.66(18)	C2-C1-C14	141.3(2)
C3-C2-C1	119.1(2)	C3-C2-H2	120.4
C1-C2-H2	120.4	C2-C3-C4	123.2(2)
C2-C3-H3	118.4	C4-C3-H3	118.4
C5-C4-C3	118.7(2)	C5-C4-H4	120.7
C3-C4-H4	120.7	N1-C5-C4	115.3(2)
N1-C5-C6	103.31(18)	C4-C5-C6	141.4(2)
C7-C6-C11	120.6(2)	C7-C6-C5	130.8(2)
C11-C6-C5	108.54(19)	C8-C7-C6	119.3(2)
C8-C7-H7	120.3	C6-C7-H7	120.3
C7-C8-C9	119.5(2)	C7-C8-H8	120.2

C9-C8-H8	120.2	C10-C9-C8	123.1(2)
C10-C9-Cl1	119.05(19)	C8-C9-Cl1	117.85(18)
C9-C10-C11	118.2(2)	C9-C10-H10	120.9
C11-C10-H10	120.9	C10-C11-C6	119.2(2)
C10-C11-C12	133.4(2)	C6-C11-C12	107.42(19)
N1-C12-C13	106.18(18)	N1-C12-C11	104.13(18)
C13-C12-C11	149.7(2)	C14-C13-C12	106.73(19)
C14-C13-Si1	130.89(17)	C12-C13-Si1	122.22(16)
C13-C14-C1	108.9(2)	C13-C14-C15	128.5(2)
C1-C14-C15	122.6(2)	C16A-C15-C14	126.4(16)
C16-C15-C14	124.0(5)	C16-C15-C17	121.6(6)
C14-C15-C17	114.4(4)	C16A-C15-C17A	121.4(17)
C14-C15-C17A	111.9(11)	C15-C16-H16A	120.0
C15-C16-H16B	120.0	H16A-C16-H16B	120.0
C15-C17-H17A	109.5	C15-C17-H17B	109.5
H17A-C17-H17B	109.5	C15-C17-H17C	109.5
H17A-C17-H17C	109.5	H17B-C17-H17C	109.5
C15-C16A-H16C	120.0	C15-C16A-H16D	120.0
H16C-C16A-H16D	120.0	C15-C17A-H17D	109.5
C15-C17A-H17E	109.5	H17D-C17A-H17E	109.5
C15-C17A-H17F	109.5	H17D-C17A-H17F	109.5
H17E-C17A-H17F	109.5	Si1-C18-H18A	109.5
Si1-C18-H18B	109.5	H18A-C18-H18B	109.5
Si1-C18-H18C	109.5	H18A-C18-H18C	109.5
H18B-C18-H18C	109.5	Si1-C19-H19A	109.5
Si1-C19-H19B	109.5	H19A-C19-H19B	109.5
Si1-C19-H19C	109.5	H19A-C19-H19C	109.5
H19B-C19-H19C	109.5	Si1-C20-H20A	109.5
Si1-C20-H20B	109.5	H20A-C20-H20B	109.5
Si1-C20-H20C	109.5	H20A-C20-H20C	109.5
H20B-C20-H20C	109.5		

Table S6. Torsion angles (º) for compound **3c**.

C12-N1-C1-C2	177.0(2)	C5-N1-C1-C2	0.1(3)
C12-N1-C1-C14	-0.2(3)	C5-N1-C1-C14	-177.1(2)
N1-C1-C2-C3	0.2(3)	C14-C1-C2-C3	175.8(3)
C1-C2-C3-C4	-0.2(4)	C2-C3-C4-C5	-0.2(4)
C12-N1-C5-C4	-177.3(2)	C1-N1-C5-C4	-0.5(3)
C12-N1-C5-C6	1.2(3)	C1-N1-C5-C6	178.0(2)

C3-C4-C5-N1	0.4(3)	C3-C4-C5-C6	-177.2(3)
N1-C5-C6-C7	179.5(2)	C4-C5-C6-C7	-2.7(5)
N1-C5-C6-C11	-0.9(2)	C4-C5-C6-C11	176.9(3)
C11-C6-C7-C8	0.2(4)	C5-C6-C7-C8	179.8(2)
C6-C7-C8-C9	0.0(4)	C7-C8-C9-C10	-0.6(4)
C7-C8-C9-Cl1	-179.77(19)	C8-C9-C10-C11	1.0(4)
Cl1-C9-C10-C11	-179.85(17)	C9-C10-C11-C6	-0.8(3)
C9-C10-C11-C12	179.5(2)	C7-C6-C11-C10	0.2(3)
C5-C6-C11-C10	-179.5(2)	C7-C6-C11-C12	-180.0(2)
C5-C6-C11-C12	0.4(3)	C1-N1-C12-C13	0.2(3)
C5-N1-C12-C13	177.49(19)	C1-N1-C12-C11	-178.35(18)
C5-N1-C12-C11	-1.0(3)	C10-C11-C12-N1	-179.9(2)
C6-C11-C12-N1	0.3(2)	C10-C11-C12-C13	3.0(6)
C6-C11-C12-C13	-176.8(4)	N1-C12-C13-C14	-0.1(2)
C11-C12-C13-C14	177.0(4)	N1-C12-C13-Si1	175.76(16)
C11-C12-C13-Si1	-7.1(5)	C20-Si1-C13-C14	122.7(2)
C18-Si1-C13-C14	4.3(3)	C19-Si1-C13-C14	-118.3(2)
C20-Si1-C13-C12	-52.0(2)	C18-Si1-C13-C12	-170.5(2)
C19-Si1-C13-C12	66.9(2)	C12-C13-C14-C1	0.0(3)
Si1-C13-C14-C1	-175.36(18)	C12-C13-C14-C15	-177.5(2)
Si1-C13-C14-C15	7.2(4)	N1-C1-C14-C13	0.1(3)
C2-C1-C14-C13	-175.8(3)	N1-C1-C14-C15	177.7(2)
C2-C1-C14-C15	1.9(5)	C13-C14-C15-C16A	-128.(2)
C1-C14-C15-C16A	55.(2)	C13-C14-C15-C16	59.7(7)
C1-C14-C15-C16	-117.4(6)	C13-C14-C15-C17	-121.7(6)
C1-C14-C15-C17	61.2(6)	C13-C14-C15-C17A	58.5(12)
C1-C14-C15-C17A	-118.6(12)		

7. Photophysical Studies

Absorption spectra were measured on a Varian Cary 100 double-beam UV-Vis-NIR spectrometer and baseline-corrected. Steady-state photoluminescence excitation and emission spectra were recorded on a FluoTime300 spectrometer from PicoQuant equipped with a 300 W ozone-free Xe lamp (250-900 nm), a 10 W Xe flash-lamp (250-900 nm, pulse width < 10 µs) with repetition rates of 0.1 – 300 Hz, an excitation monochromator (Czerny-Turner 2.7 nm/mm dispersion, 1200 grooves/mm, blazed at 300 nm), diode lasers (pulse width < 80 ps) operated by a computer-controlled laser

driver PDL-820 (repetition rate up to 80 MHz, burst mode for slow and weak decays), two emission monochromators (Czerny-Turner, selectable gratings blazed at 500 nm with 2.7 nm/mm dispersion and 1200 grooves/mm, or blazed at 1250 nm with 5.4 nm/mm dispersion and 600 grooves/mm), Glan-Thompson polarizers for excitation (Xe-lamps) and emission, a Peltier-thermostatized sample holder from Quantum Northwest (-40 °C – 105 °C), and two detectors, namely a PMA Hybrid 40 (transit time spread FWHM < 120 ps, 300 – 720 nm) and a R5509-42 NIR-photomultiplier tube (transit time spread FWHM 1.5 ns, 300-1400 nm) with external cooling (-80 °C) from Hamamatsu.

Steady-state and fluorescence lifetimes were recorded in TCSPC mode by a PicoHarp 300 (minimum base resolution 4 ps). Emission and excitation spectra were corrected for source intensity (lamp and grating) by standard correction curves. Lifetime analysis was performed using the commercial FluoFit software. The quality of the fit was assessed by minimizing the reduced chi squared function ($\chi 2$) and visual inspection of the weighted residuals and their autocorrelation. Photoluminescence quantum yields were measured with a Hamamatsu Photonics absolute PL quantum yield measurement system (C9920-02) equipped with a L9799-01 CW Xenon light source (150 W), monochromator, C7473 photonic multi-channel analyzer, integrating sphere and employing U6039-05 PLQY measurement software (Hamamatsu Photonics, Ltd., Shizuoka, Japan). All solvents used were of spectrometric grade (Uvasol®). The fluorescence rate constant (k_F) and the non-radiative deactivation rate constant (k_{NR}) according to the following equations:

$$k_F = \frac{\Phi_F}{\tau} \qquad \textit{(eq. 1)}$$

$$k_{nr} = k_{IC} + k_{ISC} \qquad \textit{(eq. 2)}$$

$$\tau = \frac{1}{k_F + k_{IC} + k_{ISC}} \qquad \textit{(eq. 3)}$$

$$k_{IC} + k_{ISC} = \frac{1 - \Phi_F}{\tau} \qquad \textit{(eq. 4)}$$

where k_{IC} is the internal conversion rate constant and k_{ISC} is the intersystem crossing rate constant.

7.1. Photoluminescence Measurements at Room Temperature

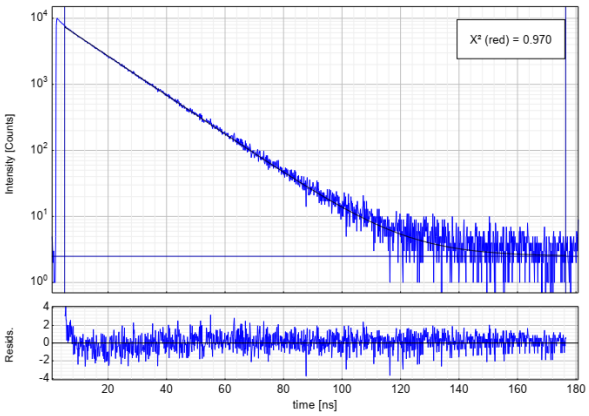

Parameter	Value	Conf. Lower	Conf. Upper	Conf. Estimation
A_1 [Cnts]	7316.1	-45.5	+45.5	Fitting
τ_1 [ns]	14.6514	-0.0661	+0.0661	Fitting
Bkgr. Dec [Cnts]	2.509	-0.517	+0.517	Fitting

Average Lifetime:

$\tau_{Av.1}$=14.6514 ns (intensity weighted)

$\tau_{Av.2}$=14.6514 ns (amplitude weighted)

Figure S3. Left: time-resolved photoluminescence decay of **3a** in an air-saturated DCM solution at 298 K, including the residuals (λ_{exc} = 310 nm, λ_{em} = 500 nm). Right: fitting parameters including pre-exponential factors and confidence limits.

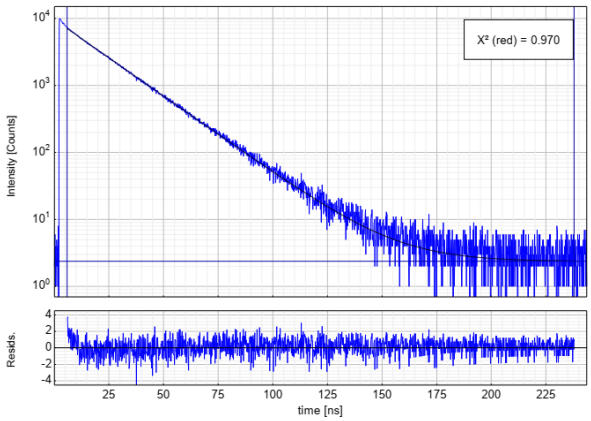

Parameter	Value	Conf. Lower	Conf. Upper	Conf. Estimation
A_1 [Cnts]	7010.4	-45.6	+45.6	Fitting
τ_1 [ns]	18.9665	-0.0896	+0.0896	Fitting
Bkgr. Dec [Cnts]	2.373	-0.485	+0.485	Fitting

Average Lifetime:

$\tau_{Av.1}$=18.9665 ns (intensity weighted)

$\tau_{Av.2}$=18.9665 ns (amplitude weighted)

Figure S4. Left: time-resolved photoluminescence decay of **3a** in an Ar-saturated DCM solution at 298 K, including the residuals (λ_{exc} = 310 nm, λ_{em} = 500 nm). Right: fitting parameters including pre-exponential factors and confidence limits.

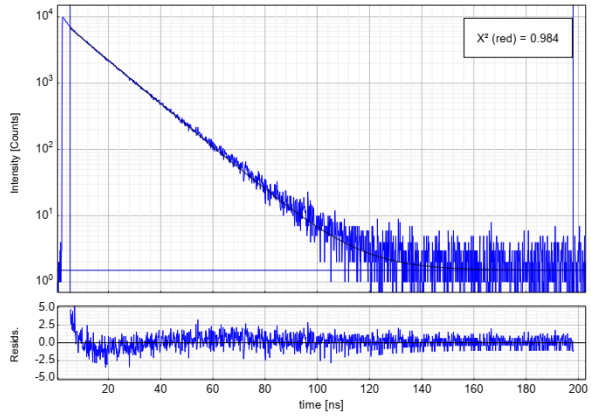

Parameter	Value	Conf. Lower	Conf. Upper	Conf. Estimation
A_1 [Cnts]	6654.6	-48.7	+48.7	Fitting
τ_1 [ns]	13.2613	-0.0708	+0.0708	Fitting
Bkgr. Dec [Cnts]	1.514	-0.383	+0.383	Fitting

Average Lifetime:

$\tau_{Av.1}$=13.2613 ns (intensity weighted)

$\tau_{Av.2}$=13.2613 ns (amplitude weighted)

Figure S5. Left: time-resolved photoluminescence decay of **3b** in an air-saturated DCM solution at 298 K, including the residuals (λ_{exc} = 310 nm, λ_{em} = 500 nm). Right: fitting parameters including pre-exponential factors and confidence limits.

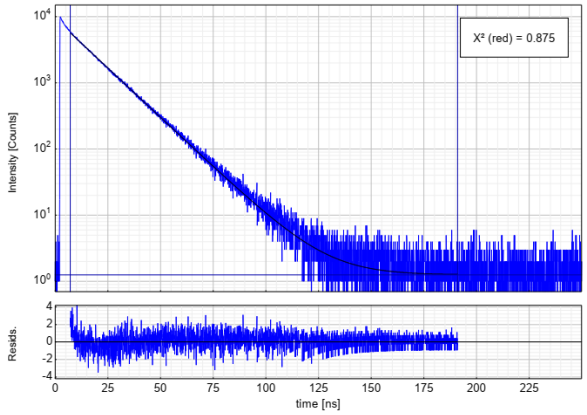

Parameter	Value	Conf. Lower	Conf. Upper	Conf. Estimation
A_1 [Cnts]	5709.3	-39.8	+39.8	Fitting
τ_1 [ns]	14.5361	-0.0735	+0.0735	Fitting
Bkgr. Dec [Cnts]	1.255	-0.377	+0.377	Fitting

Average Lifetime:

$\tau_{Av.1}$=14.5361 ns (intensity weighted)

$\tau_{Av.2}$=14.5361 ns (amplitude weighted)

Figure S6. Left: time-resolved photoluminescence decay of **3b** in an Ar-saturated DCM solution at 298 K, including the residuals (λ_{exc} = 310 nm, λ_{em} = 500 nm). Right: fitting parameters including pre-exponential factors and confidence limits.

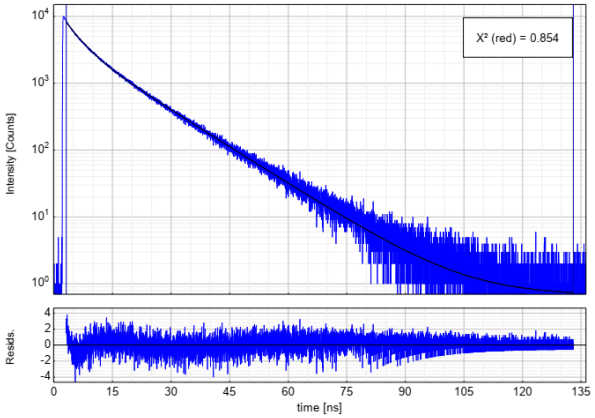

Parameter	Value	Conf. Lower	Conf. Upper	Conf. Estimation
A_1 [Cnts]	3845.3	-34.2	+34.2	Fitting
τ_1 [ns]	11.8293	-0.0687	+0.0687	Fitting
A_2 [Cnts]	4330.0	-91.4	+91.4	Fitting
τ_2 [ns]	3.7729	-0.0835	+0.0835	Fitting
Bkgr. Dec [Cnts]	0.675	-0.371	+0.371	Fitting

Average Lifetime:

$\tau_{Av.1}$=9.7004 ns (intensity weighted)

$\tau_{Av.2}$=7.5623 ns (amplitude weighted)

Figure S7. Left: time-resolved photoluminescence decay of **3c** in an air-saturated DCM solution at 298 K, including the residuals (λ_{exc} = 310 nm, λ_{em} = 500 nm). Right: fitting parameters including pre-exponential factors and confidence limits.

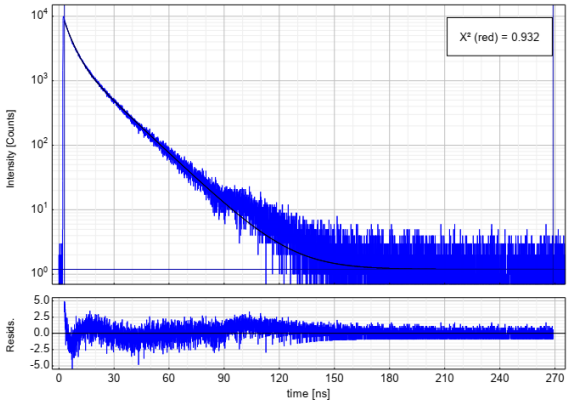

Parameter	Value	Conf. Lower	Conf. Upper	Conf. Estimation
A_1 [Cnts]	2540.8	-37.1	+37.1	Fitting
τ_1 [ns]	16.153	-0.149	+0.149	Fitting
A_2 [Cnts]	5789	-125	+125	Fitting
τ_2 [ns]	4.3199	-0.0942	+0.0942	Fitting
Bkgr. Dec [Cnts]	1.191	-0.316	+0.316	Fitting

Average Lifetime:

$\tau_{Av.1}$=11.673 ns (intensity weighted)

$\tau_{Av.2}$=7.929 ns (amplitude weighted)

Figure S8. Left: time-resolved photoluminescence decay of **3c** in an Ar-saturated DCM solution at 298 K, including the residuals (λ_{exc} = 310 nm, λ_{em} = 500 nm). Right: fitting parameters including pre-exponential factors and confidence limits.

7.2. Photoluminescence Measurements at Low Temperature

The emission spectra of compounds **3a**, **3b** and **3c** at low temperature were also measured and are illustrated in Figure S9. In the glassy matrix (DCM:MeOH 1:1) at 77 K, where solvatochromic stabilization by interaction with the fluid environment is diminished, all the molecules show a blue shift with respect to room temperature, yielding λ_{max} **3a** = 488 nm, λ_{max} **3b** = 470 nm and λ_{max} **3c** = 483 nm; and in all cases, a small vibrational shoulder arises. As observed, the substituent-dependent blue shift remains the same as at room temperature. The photophysical properties of these compounds were also measured at low temperature (Table S6).

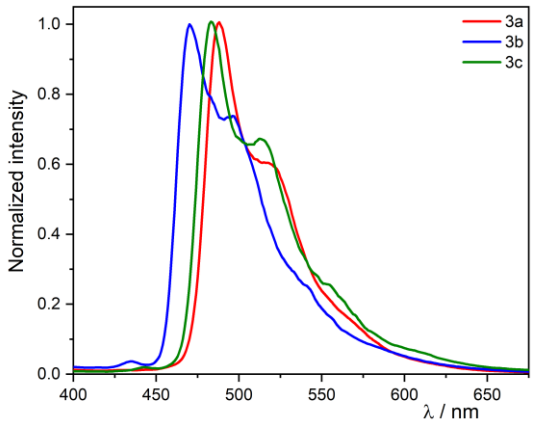

Figure S9. Photoluminescence spectra (bold) of **3a** (red), **3b** (blue) and **3c** (green) (λ_{exc} = 325 nm) at 77 K in a DCM:MeOH 1:1 frozen glassy matrix. All solutions were optically diluted (A < 0.1). The spectra are normalized to the highest intensity.

Table S7. Fluorescence quantum yields (Φ_F), excited state luminescence lifetimes (τ), radiative (k_F) and non-radiative deactivation rate constants (k_{NR}) of the compounds in a DCM:MeOH frozen glassy matrix at 77K. *Calculated using the amplitude-weighted average lifetime (τ_{av_amp}).

Sample	3a	3b	3c
$\Phi_{F\ (77K)}$ ± 4 / %	95	67	71
$\tau_{(77K)}$ / ns		τ_1 = 24.20 ± 0.12 (77%); τ_2 = 11.4 ± 0.3 (23%) τ_{av_amp} = 19.2 ± 0.8	τ_1 = 18.8 ± 0.1 (60%); τ_2 = 5.3 ± 0.2 (40%) τ_{av_amp} = 13.4 ± 0.6	τ_1 = 16.20 ± 0.11 (49%); τ_2 = 4.80 ± 0.14 (51%) τ_{av_amp} = 10.3 ± 0.6
k_F / 10^6 s^{-1}		5.1 ± 0.5*	5.0 ± 0.6*	6.9 ± 0.8*
k_{NR} / 10^6 s^{-1}		0.015 ± 0.005*	1.7 ± 0.9*	2.8 ± 0.3*

In a frozen glassy matrix at 77 K, charge transfer states are destabilized, lowering the n-π character of the S_1. Therefore, the emission at 77 K is originated mostly from π-π states. This effect is verified by the values of k_F, which are similar in all cases, as opposed to room temperature. As depicted in Table 2, Φ_F for **3a** is close to unity, hence k_{NR} is almost insignificant. Instead, for **3b** and **3c**, the higher k_{NR} (yet comparable) values are caused by enhanced densities of vibrational states due to the presence of the added substituents that favour radiationless deactivation pathways (k_{IC}).

Time-resolved photoluminescence decay curves:

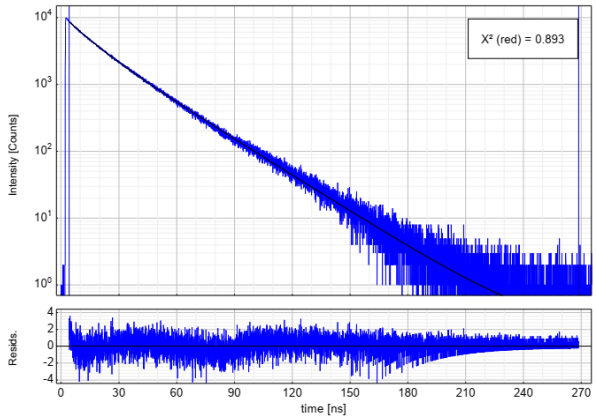

Parameter	Value	Conf. Lower	Conf. Upper	Conf. Estimation
A_1 [Cnts]	5243.1	-40.4	+40.4	Fitting
τ_1 [ns]	24.206	-0.121	+0.121	Fitting
A_2 [Cnts]	3357.0	-78.0	+78.0	Fitting
τ_2 [ns]	11.384	-0.265	+0.265	Fitting
Bkgr. Dec [Cnts]	0.212	-0.376	+0.376	Fitting

Average Lifetime:

$\tau_{Av.1}$=21.239 ns (intensity weighted)

$\tau_{Av.2}$=19.201 ns (amplitude weighted)

Figure S10. Left: time-resolved photoluminescence decay of **3a** in a frozen glassy matrix of DCM/MeOH (V:V = 1:1) at 77 K, including the residuals (λ_{exc} = 317 nm, λ_{em} = 490 nm). Right: fitting parameters including pre-exponential factors and confidence limits.

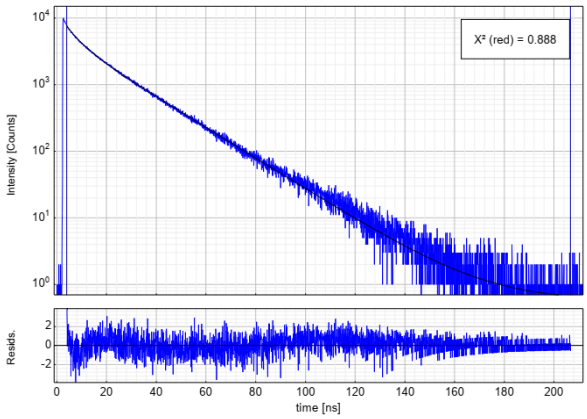

Parameter	Value	Conf. Lower	Conf. Upper	Conf. Estimation
A_1 [Cnts]	4469.5	-35.2	+35.2	Fitting
τ_1 [ns]	18.796	-0.100	+0.100	Fitting
A_2 [Cnts]	2948.2	-97.0	+97.0	Fitting
τ_2 [ns]	5.273	-0.194	+0.194	Fitting
Bkgr. Dec [Cnts]	0.577	-0.385	+0.385	Fitting

Average Lifetime:

$\tau_{Av.1}$=16.685 ns (intensity weighted)

$\tau_{Av.2}$=13.421 ns (amplitude weighted)

Figure S11. Left: time-resolved photoluminescence decay of **3b** in a frozen glassy matrix of DCM/MeOH (V:V = 1:1) at 77 K, including the residuals (λ_{exc} = 317 nm, λ_{em} = 470 nm). Right: fitting parameters including pre-exponential factors and confidence limits.

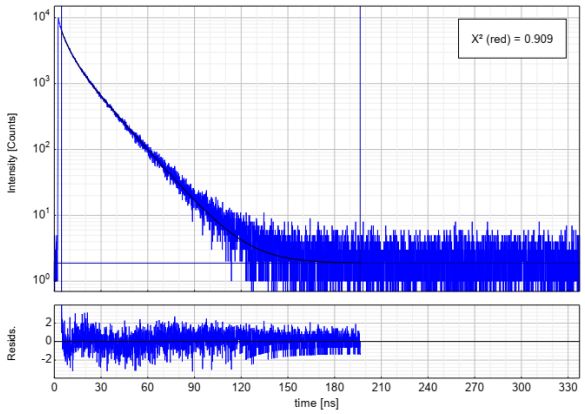

Parameter	Value	Conf. Lower	Conf. Upper	Conf. Estimation
A_1 [Cnts]	3030.0	-32.1	+32.1	Fitting
τ_1 [ns]	16.122	-0.114	+0.114	Fitting
A_2 [Cnts]	3195.4	-88.8	+88.8	Fitting
τ_2 [ns]	4.836	-0.144	+0.144	Fitting
Bkgr. Dec [Cnts]	1.882	-0.413	+0.413	Fitting

Average Lifetime:

$\tau_{Av.1}$=13.409 ns (intensity weighted)

$\tau_{Av.2}$=10.329 ns (amplitude weighted)

Figure S12. Left: time-resolved photoluminescence decay of **3c** in a frozen glassy matrix of DCM/MeOH (V:V = 1:1) at 77 K, including the residuals (λ_{exc} = 317 nm, λ_{em} = 470 nm). Right: fitting parameters including pre-exponential factors and confidence limits.

8. Computational Study

8.1. Computational Details

Ground-state calculations were performed in the DFT framework with the Gaussian 09 Rev. D.01 quantum chemistry package.[5] The B3LYP hybrid functional[6] with a 6-31+G* basis set was used. Van-der-Waals interactions were approximatively included by Grimme-D3 dispersion corrections with Becke-Johnson damping (BJ).[7] Solvent effects were taken into account using the polarizable continuum model (PCM)[8] with UFF atomic radii[9] for dichloromethane. Absorption spectra were obtained from time-dependent density functional linear response theory (TDDFT) calculations of the lowest 40 singlet excited states and broadened by Lorentzian distributions with a half-width at half-maximum (HWHM) of 10 nm. Emission energies were determined from the TDDFT optimized S1 geometry. Structures and orbitals were visualized using Avogadro.[10] All output files are provided as an electronic supplement.

8.2. Calculated Absorption Spectra

The calculated absorption spectra of the INIs **3a**, **3b** and **3c** in dichloromethane are shown in Figure S13.

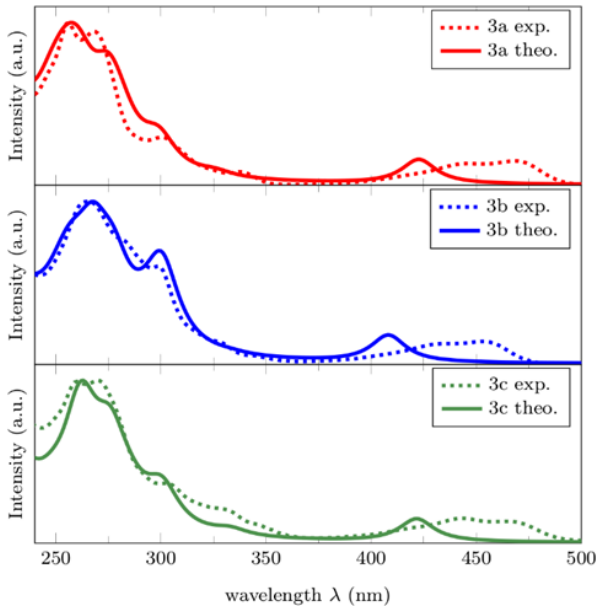

Figure S13. Normalized calculated (theo., solid lines) and experimental (exp., dashed lines) UV-vis absorption spectra of **3a**, **3b**, and **3c** in dichloromethane. Theoretical spectra were calculated using TDDFT with the B3LYP functional and 6-31+G* basis set.

8.3. Optimized Geometries

Table S8. Optimized geometries in the ground state (GS) and first excited state (S_1) of compounds **3a**, **3b** and **3c** calculated with Gaussian 09 Rev. D.01[5] and B3LYP with 6-31+G* basis.

Sample	3a	3b	3c
GS	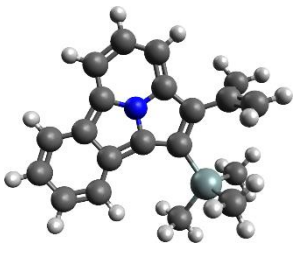	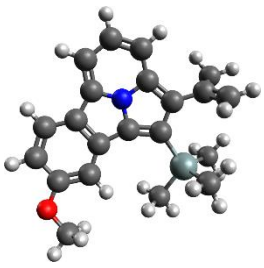	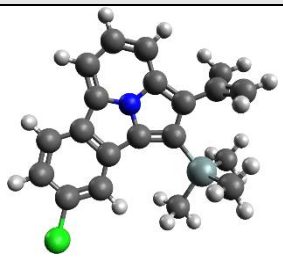
S1	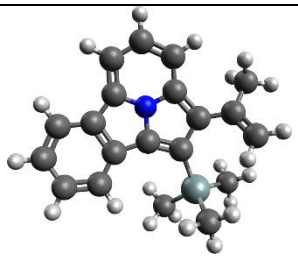	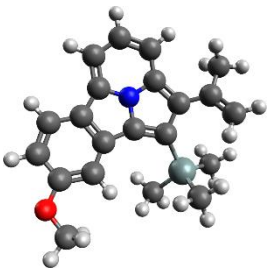	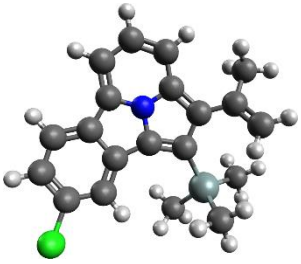

Table S9. Selected bond lengths (in Å), angles and dihedrals (in degrees) of the optimized geometries in ground state (GS) and first excited state (S_1) of compounds **3a**, **3b** and **3c** calculated with Gaussian 09 Rev. D.01[5] and B3LYP with 6-31+G* basis. The atom labels are shown in Figure S2.

Sample	3a GS	3a S1	3b GS	3b S1	3cGS	3c S1
N1 C1	1.376	1.349	1.375	1.352	1.376	1.349
N1 C5	1.375	1.368	1.376	1.366	1.375	1.368
N1 C12	1.368	1.412	1.367	1.412	1.369	1.411
C14 C15	1.483	1.442	1.483	1.440	1.483	1.441
C15 C16	1.342	1.361	1.342	1.363	1.341	1.362
C15 C17	1.511	1.515	1.511	1.514	1.511	1.514
C13 C14	1.431	1.469	1.431	1.473	1.429	1.471
C12 C13	1.429	1.402	1.429	1.404	1.430	1.399
C1 C14	1.426	1.457	1.426	1.457	1.427	1.458
C8 C9	1.410	1.409	1.416	1.414	1.407	1.405
C13 Si1	1.888	1.888	1.888	1.885	1.890	1.890
C13 C14 C15	128.0	127.4	128.0	127.3	128.0	127.4
C16 C15 C17	122.1	119.5	122.1	119.3	122.1	119.4
Si1 C13 C14	124.6	129.2	124.6	129.3	124.7	129.5
C1 C14 C15 C16	114.7	148.8	115.0	150.4	114.6	149.2
C13 C14 C15 C17	114.1	158.6	114.3	160.8	114.0	159.3
Si1 C13 C14 C15	-5.2	-24.5	-5.1	-25.9	-5.1	-24.2
C11 C12 C13 C14	-177.8	-175.6	-178.0	-175.0	-177.9	-175.5
N1 C1 C14 C15	-179.6	-170.9	-180.0	-170.3	179.7	-170.7

8.4. Kohn-Sham Orbitals

Table S10. Molecular frontier orbitals of compounds **3a**, **3b** and **3c** at the S_0 geometry calculated with Gaussian 09 Rev. D.01[5] and B3LYP with 6-31+G* basis.

Sample	3a	3b	3c
HOMO-2	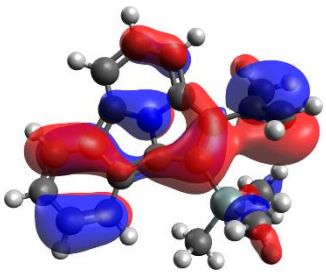	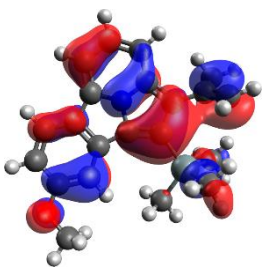	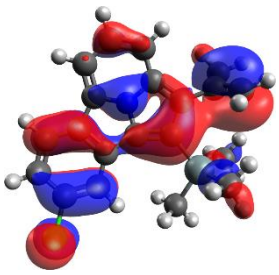

HOMO-1	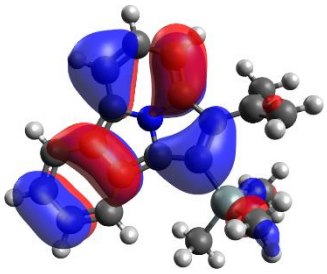	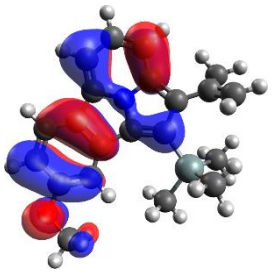	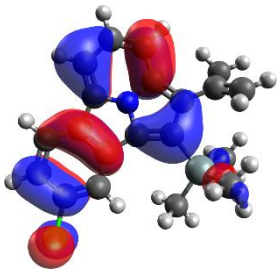
HOMO	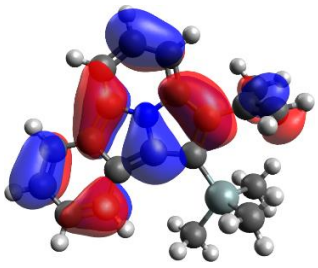	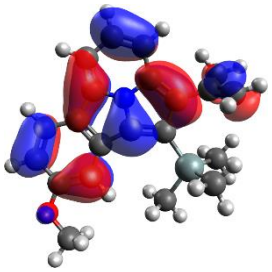	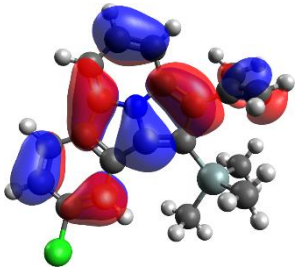
LUMO	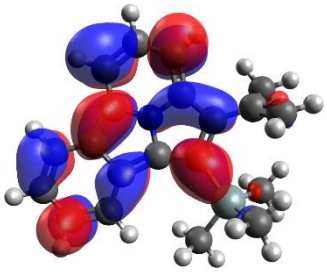	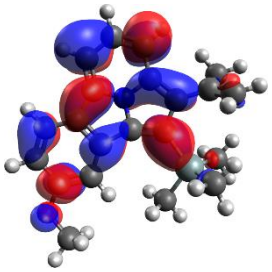	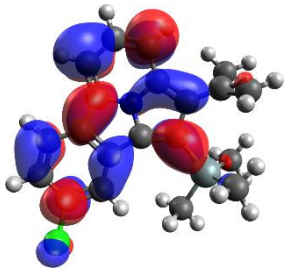
LUMO+1	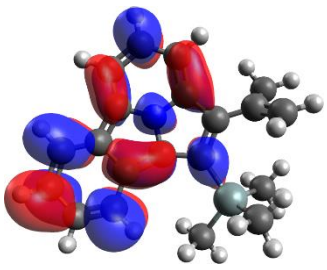	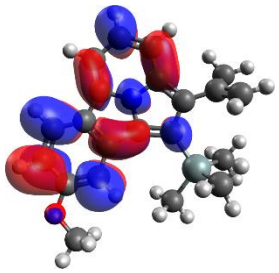	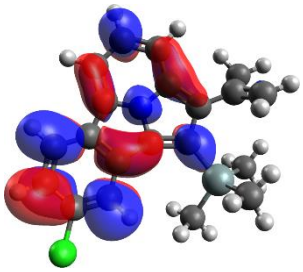
LUMO+2	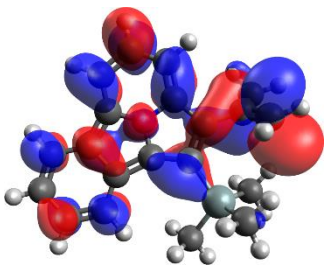	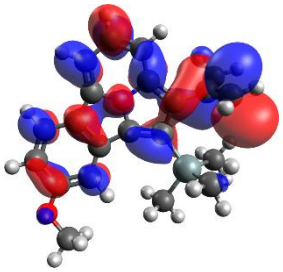	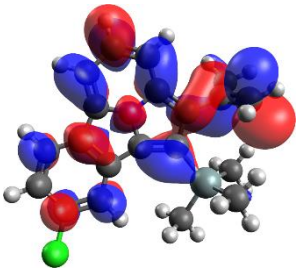
LUMO+3	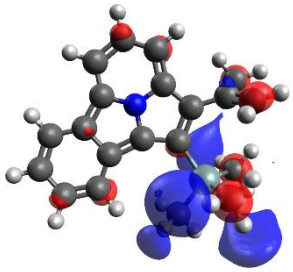	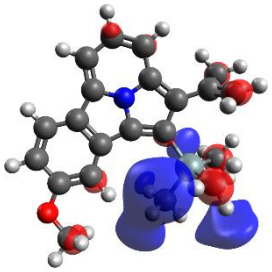	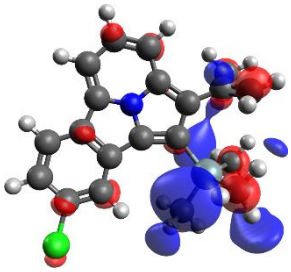

LUMO+4	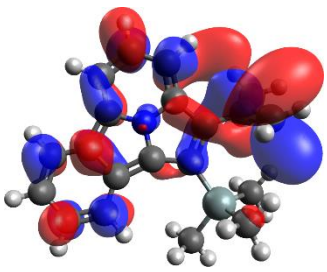	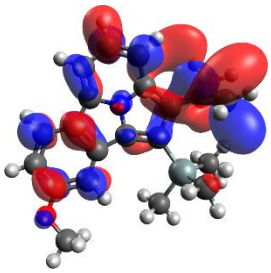	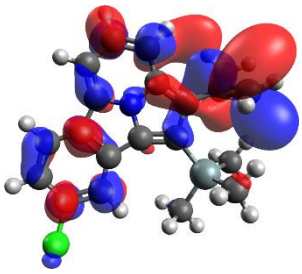

Table S11. Molecular frontier orbitals of the S_1 excited state geometry of compounds **3a**, **3b** and **3c** calculated with Gaussian 09 Rev. D.01[5] and B3LYP with 6-31+G* basis.

Sample	3a (S1 geometry)	3b (S1 geometry)	3c (S1 geometry)
HOMO-2	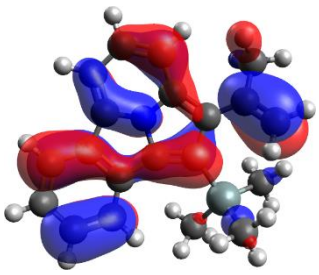	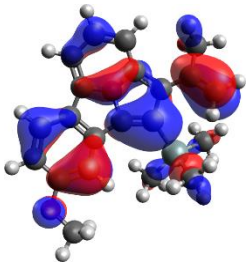	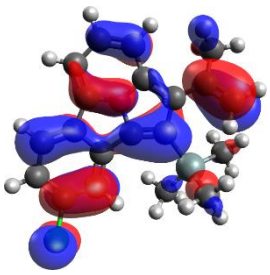
HOMO-1	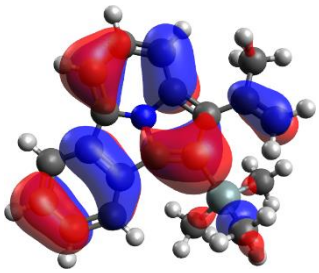	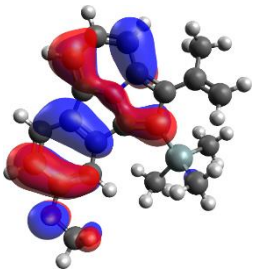	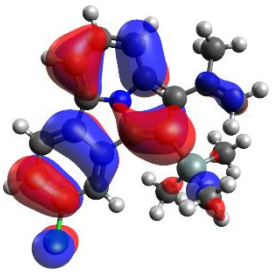
HOMO	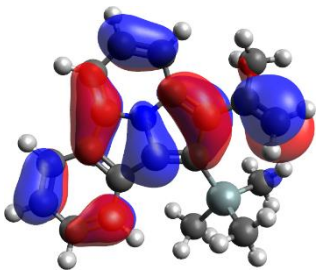	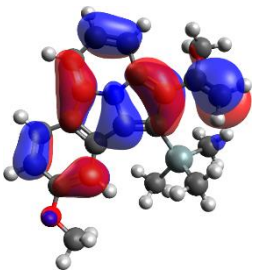	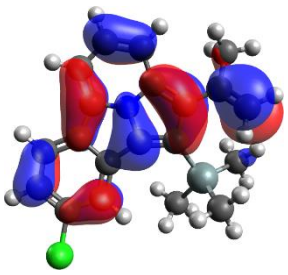
LUMO	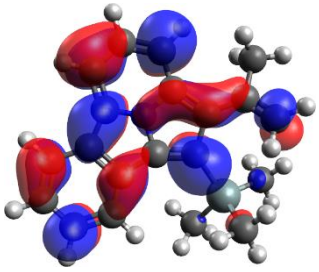	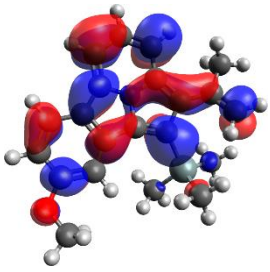	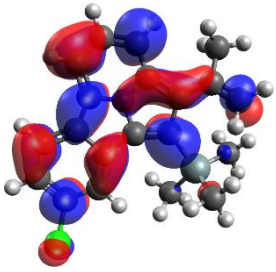

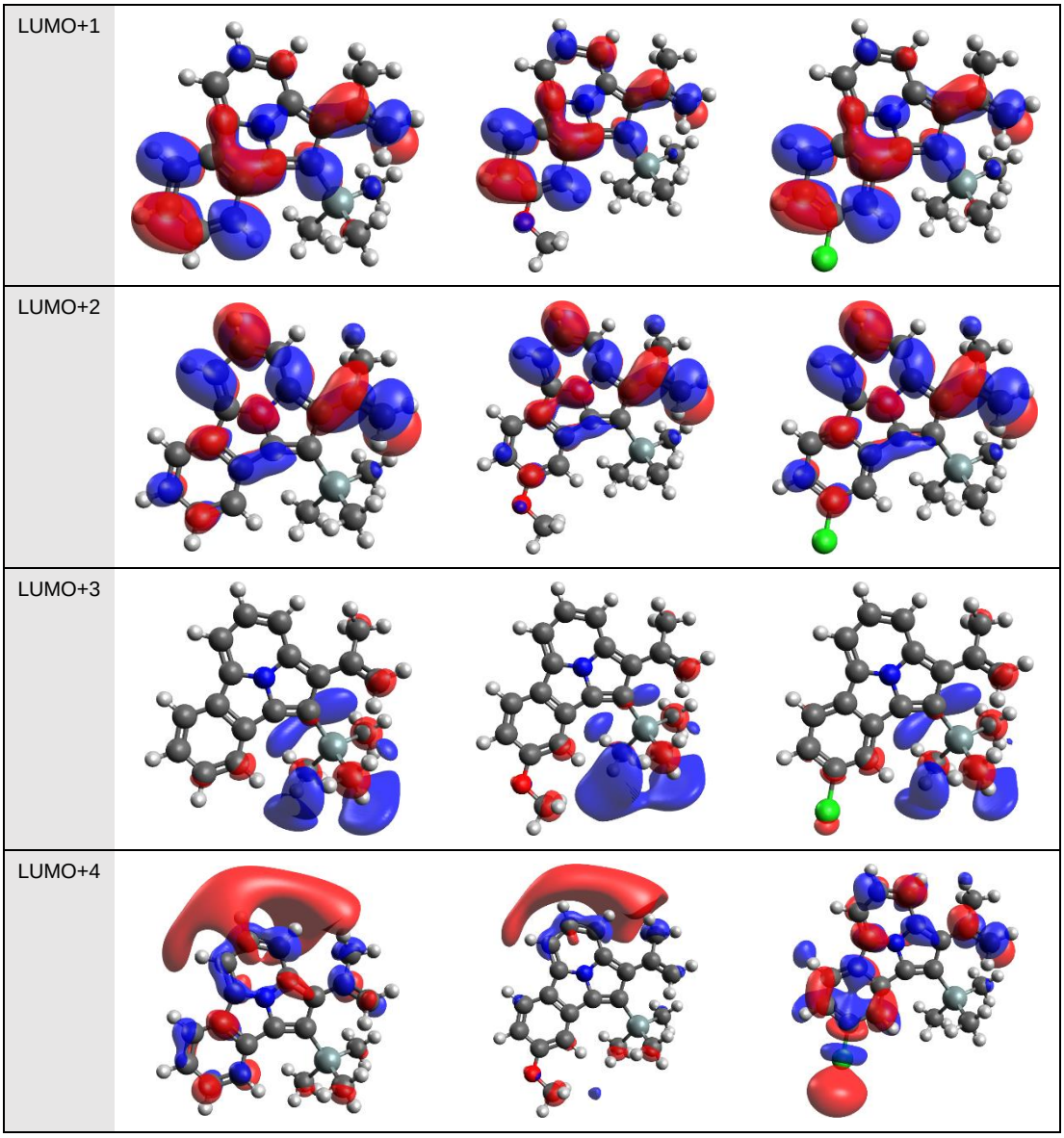

8.5. Singlet Excitations

Table S12. Calculated excitation wavelengths in nm (larger than 261 nm) and oscillator strengths for excited states of compounds **3a**, **3b** and **3c**. Contributions to the TDDFT eigenvectors larger than 10% are given for each excitation.

Sample	3a	3b	3c
1.	423 nm, f=0.137	408 nm, f=0.144	422 nm, f=0.142
	HOMO→LUMO 97%	HOMO→LUMO 95%	HOMO→LUMO 97%
2.	326 nm, f=0.028	334 nm, f=0.008	333 nm, f=0.040
	HOMO→LUMO+1 72%	HOMO→LUMO+1 52%	HOMO→LUMO+1 77%
	HOMO-1→LUMO 26%	HOMO-1→LUMO 46%	HOMO-1→LUMO 21%
3.	299 nm, f=0.182	301 nm, f=0.461	301 nm, f=0.261
	HOMO→LUMO+2 60%	HOMO→LUMO+1 36%	HOMO→LUMO+2 45%

	HOMO-1→LUMO 22% HOMO→ LUMO+1 11%	HOMO-1→LUMO 31% HOMO→LUMO+2 28%	HOMO-1→LUMO 36% HOMO→LUMO+1 11%
4.	281 nm, f=0.140 HOMO-2→LUMO 50% HOMO→LUMO+2 18% HOMO→LUMO+4 14%	293 nm, f=0.040 HOMO-2→LUMO 41% HOMO→LUMO+2 38% HOMO-1→LUMO+1 13%	285 nm, f=0.096 HOMO-2→LUMO 78% HOMO-1→LUMO+1 14%
5.	275 nm, f=0.348 HOMO-2→LUMO 33% HOMO-1→LUMO 24% HOMO→LUMO+4 17%	278 nm, f=0.311 HOMO→LUMO+4 25% HOMO→LUMO+2 21% HOMO-2→LUMO 17% HOMO-1→LUMO+1 14% HOMO-1→LUMO 10%	276 nm, f=0.460 HOMO→LUMO+2 37% HOMO-1→LUMO 27% HOMO→LUMO+4 22%
6.	271 nm, f=0.001 HOMO→LUMO+3 88%	273 nm, f=0.000 HOMO→LUMO+3 89%	266 nm, f=0.001 HOMO→LUMO+3 78%
7.	262 nm, f=0.294 HOMO→LUMO+4 45% HOMO-3→LUMO 23% HOMO-1→LUMO 12%	268 nm, f=0.446 HOMO-1→LUMO+1 60% HOMO-2→LUMO 22%	263 nm, f=0.002 HOMO-3→LUMO 75% HOMO-1→LUMO+1 12%
8.	261 nm, f=0.111 HOMO-3→LUMO 67% HOMO→LUMO+4 13%		262 nm, f=0.309 HOMO-1→LUMO+1 45% HOMO-3→LUMO 15%
9.			262 nm, f=0.435 HOMO→LUMO+4 56% HOMO-1→LUMO+1 14%

Table S13. Calculated excitation wavelengths in nm (larger than 263 nm) and oscillator strengths for excited states of the S_1-geometry of compounds **3a**, **3b** and **3c**. Contributions to the TDDFT eigenvectors larger than 10% are given for each excitation.

Sample	3a (S1 geometry)	3b (S1 geometry)	3c (S1 geometry)
1.	513 nm, f=0.139 HOMO→LUMO 98%	494 nm, f=0158 HOMO→LUMO 96%	515 nm, f=0.143 HOMO→LUMO 97%
2.	356 nm, f=0.054 HOMO→LUMO+1 73% HOMO-1→LUMO 19%	362 nm, f=0.008 HOMO→LUMO+1 53% HOMO-1→LUMO 39%	366 nm, f=0.074 HOMO→LUMO+1 84% HOMO-1→LUMO 12%
3.	336 nm, f=0.192 HOMO→LUMO+2 45% HOMO-1→LUMO 29% HOMO→LUMO+1 23%	339 nm, f=0.339 HOMO→LUMO+1 42% HOMO→LUMO+2 29% HOMO-1→LUMO 25%	337 nm, f=0.197 HOMO→LUMO+2 46% HOMO-1→LUMO 38% HOMO→LUMO+1 12%
4.	310 nm, f=0.186 HOMO-2→LUMO 56% HOMO-1→LUMO 19%	316 nm, f=0.097 HOMO-2→LUMO 60% HOMO→LUMO+2 17%	312 nm, f=0.135 HOMO-2→LUMO 77%

	HOMO→LUMO+2 18%	HOMO-1→LUMO 10%	
5.	292 nm, f=0.509 HOMO-2→LUMO 32% HOMO-1→LUMO 27% HOMO→LUMO+2 25%	301 nm, f=0.489 HOMO→LUMO+2 40% HOMO-2→LUMO 28% HOMO-1→LUMO 21%	296 nm, f=0.621 HOMO-1→LUMO 39% HOMO→LUMO+2 37% HOMO-2→LUMO 12%
6.	288 nm, f=0.031 HOMO→LUMO+3 91%	290 nm, f=0.008 HOMO→LUMO+3 93%	284 nm, f=0.010 HOMO→LUMO+3 93%
7.	268 nm, f=0.022 HOMO→LUMO+4 52% HOMO→LUMO+5 16% HOMO→LUMO+6 14%	275 nm, f=0.284 HOMO-1→LUMO+1 72%	273 nm, f=0.015 HOMO→LUMO+4 35% HOMO-1→LUMO+1 29% HOMO→LUMO+5 19%
8.	264 nm, f=0.014 HOMO→LUMO+4 42% HOMO→LUMO+5 26%	267 nm, f=0.022 HOMO→LUMO+4 90%	267 nm, f=0.397 HOMO-1→LUMO+1 44% HOMO→LUMO+4 28% HOMO→LUMO+5 11%
9.	263 nm, f=0.183 HOMO-1→LUMO+1 36% HOMO→LUMO+5 29% HOMO-4→LUMO 14%	263 nm, f=0.148 HOMO-1→LUMO+2 42% HOMO→LUMO+6 34%	264 nm, f=0.003 HOMO→LUMO+5 64% HOMO→LUMO+4 29%

9. References

(1) G. R. Fulmer, A. J. M. Miller, N. H. Sherden, H. E. Gottlieb, A. Nudelman, B. M. Stoltz, J. E. Bercaw and K. I. Goldberg, *Organometallics,* 2010, **29**, 2176-2179.

(2) B. Zhou, H. Chen and C. Wang, *J. Am. Chem. Soc.,* 2013, **135**, 1264-1267.

(3) Y. Kitamura, S. Sako, T. Udzu, A. Tsutsui, T. Maegawa, Y. Monguchi and H. Sajiki, *Chem. Commun*., 2007, 5069-5071.

(4) P. J. Stang and T. E. Fisk, *Synthesis*, 1979, **6**, 438-440.

(5) Gaussian 09, Revision D.01, M. J. Frisch, G. W. Trucks, H. B. Schlegel, G. E. Scuseria, M. A. Robb, J. R. Cheeseman, G. Scalmani, V. Barone, B. Mennucci, G. A. Petersson, H. Nakatsuji, M. Caricato, X. Li, H. P. Hratchian, A. F. Izmaylov, J. Bloino, G. Zheng, J. L. Sonnenberg, M. Hada, M. Ehara, K. Toyota, R. Fukuda, J. Hasegawa, M. Ishida, T. Nakajima, Y. Honda, O. Kitao, H. Nakai, T. Vreven, J. A. Montgomery, Jr., J. E. Peralta, F. Ogliaro, M. Bearpark, J. J. Heyd, E. Brothers, K. N. Kudin, V. N. Staroverov, T. Keith, R. Kobayashi, J. Normand, K. Raghavachari, A. Rendell, J. C. Burant, S. S. Iyengar, J. Tomasi, M. Cossi, N. Rega, J. M. Millam, M. Klene, J. E. Knox, J. B. Cross, V. Bakken, C. Adamo, J. Jaramillo, R. Gomperts, R. E. Stratmann, O. Yazyev, A. J. Austin, R. Cammi, C. Pomelli, J. W. Ochterski, R. L. Martin, K. Morokuma, V. G. Zakrzewski, G. A. Voth, P. Salvador, J. J. Dannenberg, S. Dapprich, A. D. Daniels, O. Farkas, J. B. Foresman, J. V. Ortiz, J. Cioslowski and D. J. Fox, *Gaussian, Inc., Wallingford CT*, 2013.

(6) A. D. Becke, *J. Chem. Phys.,* 1993, **98**, 5648-5652.

(7) S. Grimme, S. Ehrlich and L. Goerigk, *J. Comput. Chem*., 2011, **32**, 1456-1465.

(8) J. Tomasi, B. Mennucci and R. Cammi, *Chem. Rev.,* 2005,**105**, 2999-3094.
(9) A. K. Rappe, C. J. Casewit, K. S. Colwell, W. A. Goddard and W. M. Skiff, *J. Am. Chem. Soc.,* 1992, **114,** 10024-10035.
(10) Avogadro: an open-source molecular builder and visualization tool. Version 1.1.1 http://avogadro.cc/

10. NMR Spectra of Products

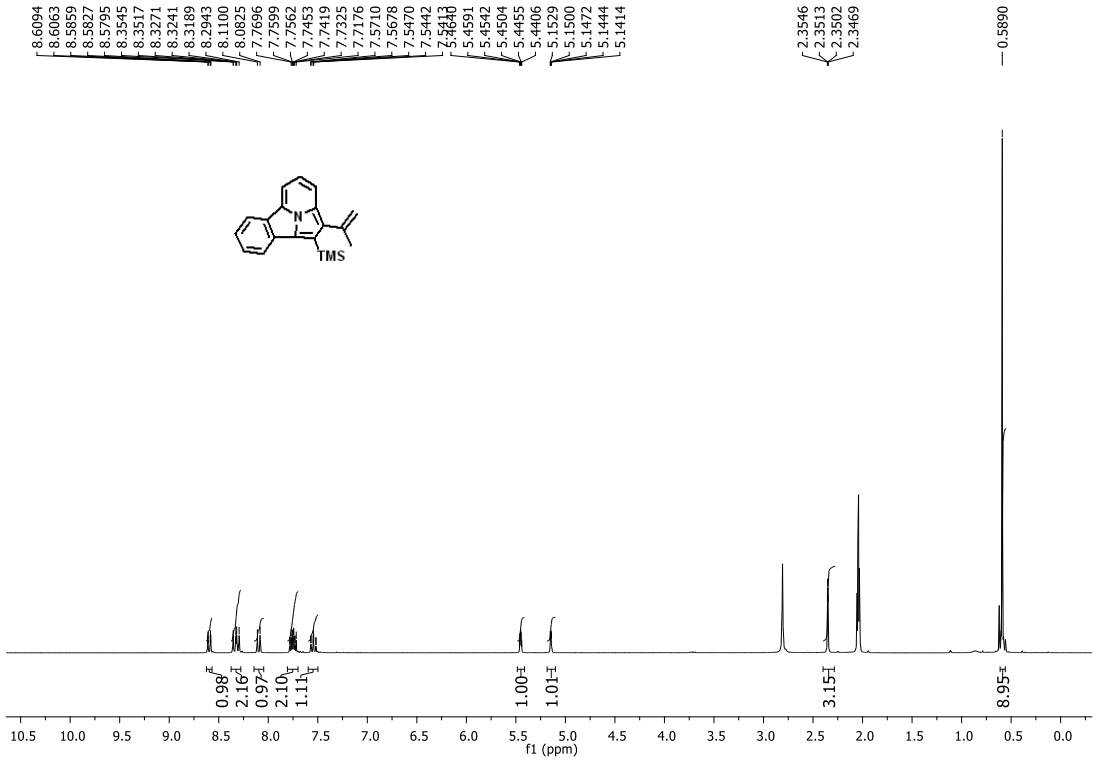

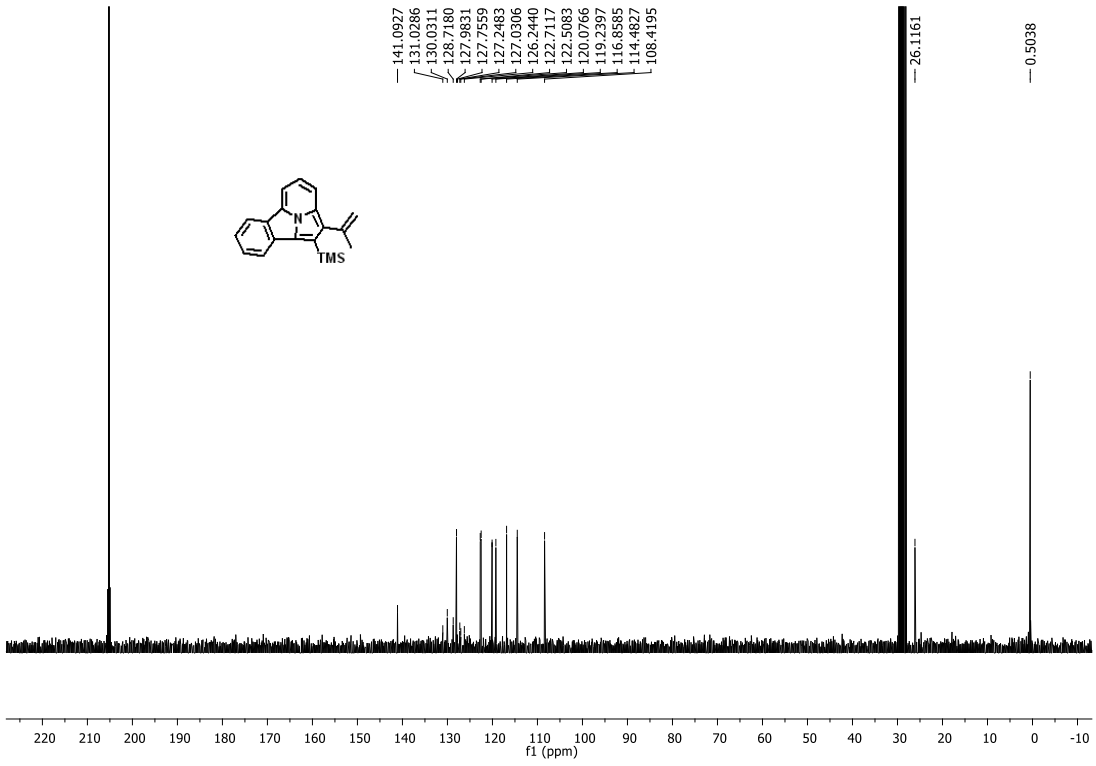

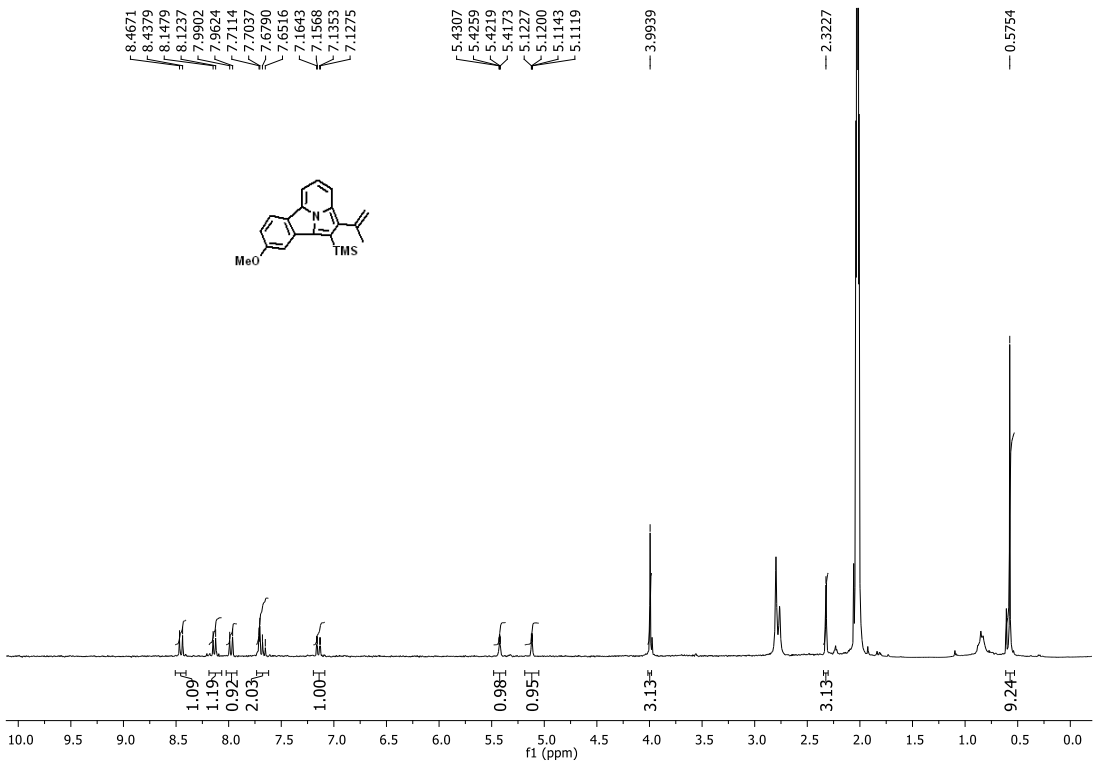
8.4671
8.4379
8.1479
8.1237
7.9902
7.9624
7.7114
7.7037
7.6790
7.6516
7.1643
7.1568
7.1353
7.1275
5.4307
5.4259
5.4219
5.4173
5.1227
5.1200
5.1143
5.1119
3.9939
2.3227
0.5754
MeO
TMS
1.09
1.19
0.92
2.03
1.00
0.98
0.95
3.13
3.13
9.24
f1 (ppm)

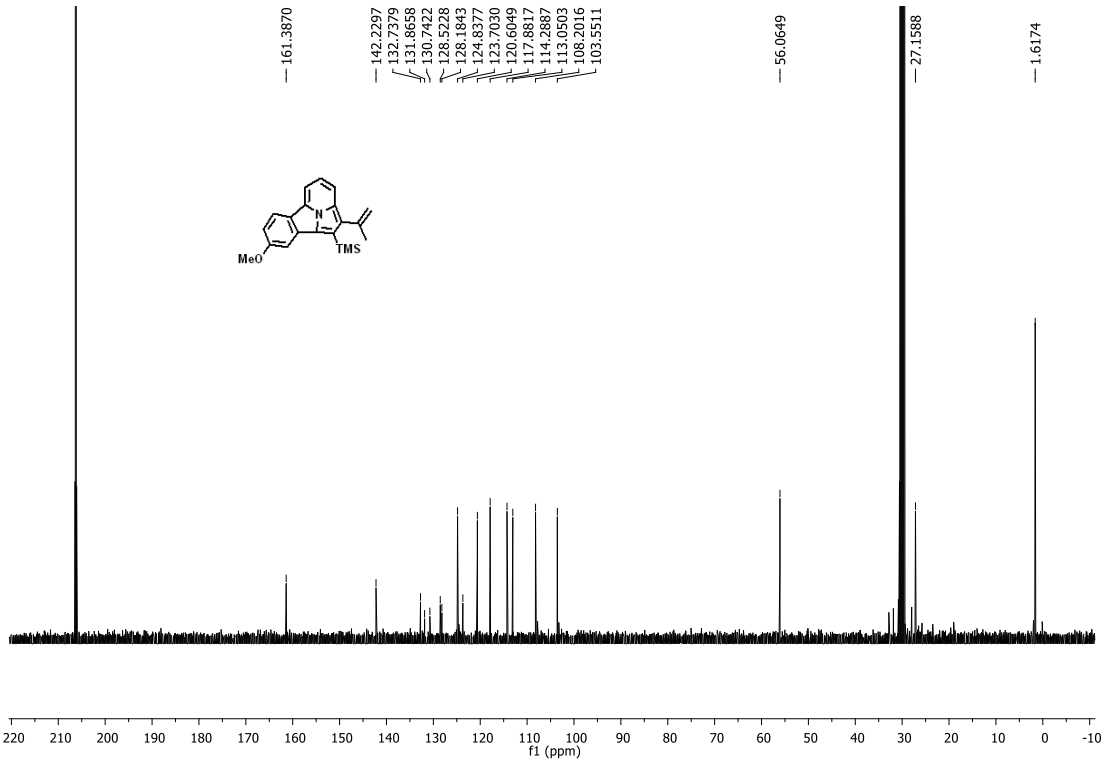
161.3870
142.2297
132.7379
131.8658
130.7422
128.5228
128.1843
124.8377
123.7030
120.6049
117.8817
114.2887
113.0503
108.2016
103.5511
56.0649
27.1588
1.6174
MeO
TMS
f1 (ppm)

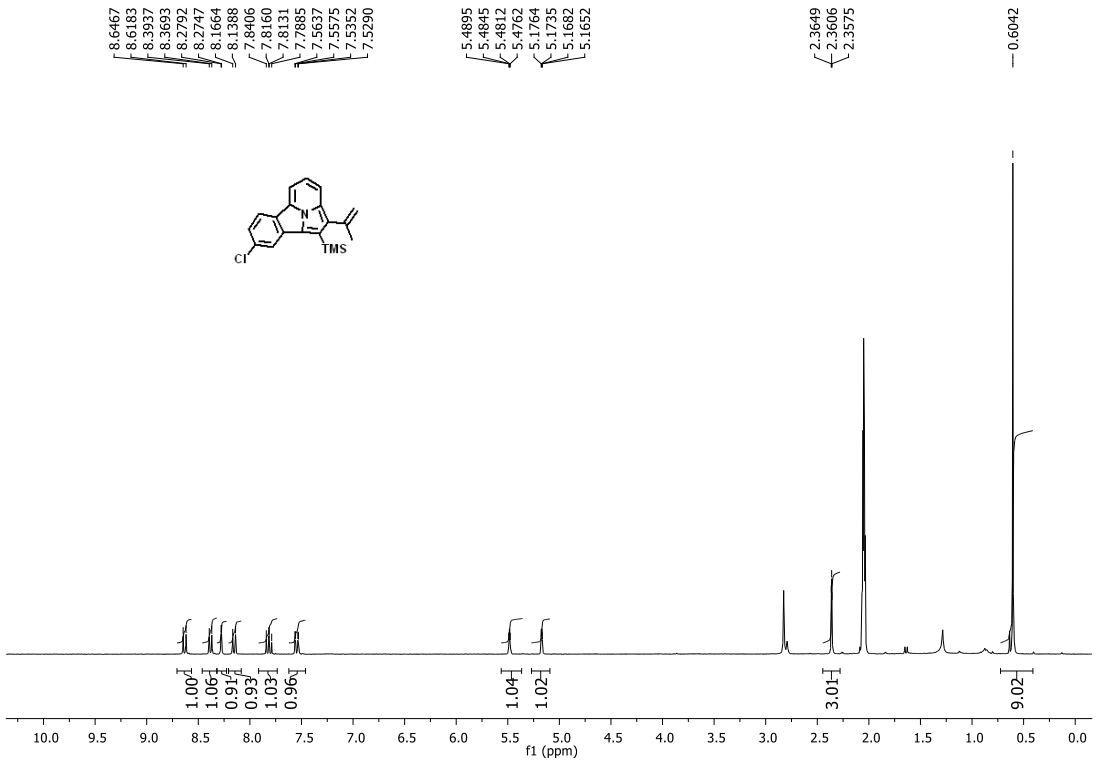
8.6467
8.6183
8.3937
8.3693
8.2792
8.2747
8.1664
8.1388
7.8406
7.8160
7.8131
7.7885
7.5637
7.5575
7.5352
7.5290
5.4895
5.4845
5.4812
5.4762
5.1764
5.1735
5.1682
5.1652
2.3649
2.3606
2.3575
0.6042
Cl
TMS
1.00
1.06
0.91
0.93
1.03
0.96
1.04
1.02
3.01
9.02
f1 (ppm)

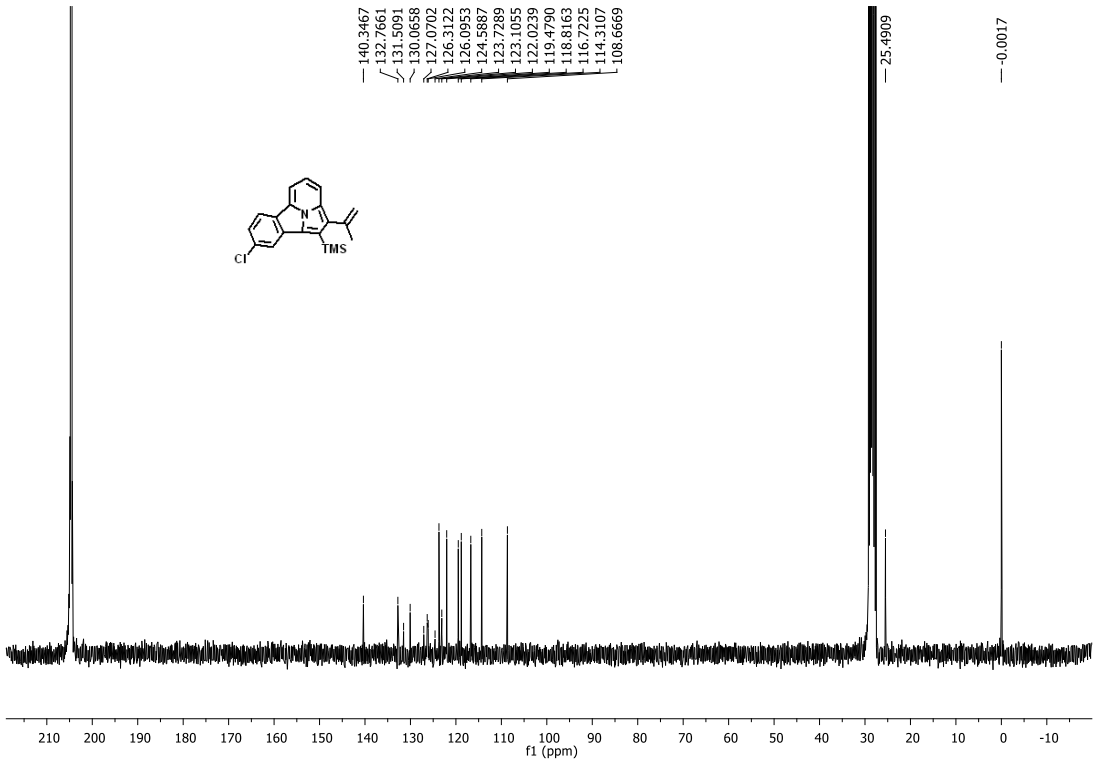
140.3467
132.7661
131.5091
130.0658
127.0702
126.3122
126.0953
124.5887
123.7289
123.1055
122.0239
119.4790
118.8163
116.7225
114.3107
108.6669
25.4909
-0.0017
Cl
TMS
f1 (ppm)

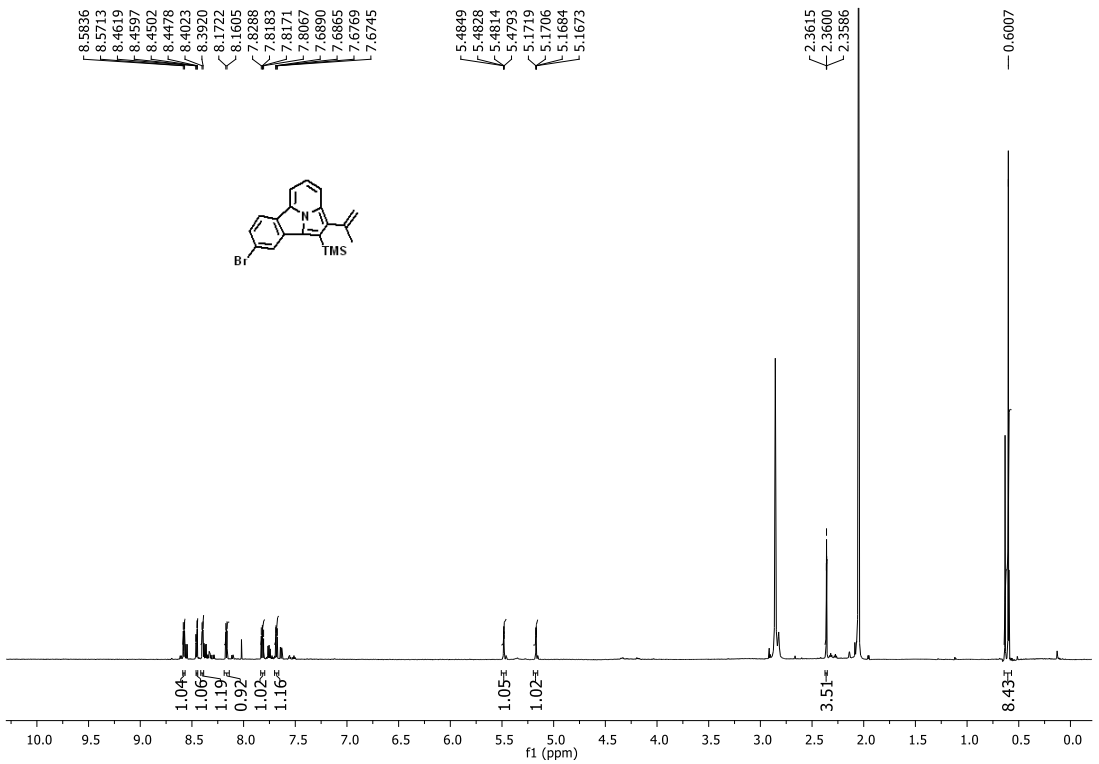
8.5836
8.5713
8.4619
8.4597
8.4502
8.4478
8.4023
8.3920
8.1722
8.1605
7.8288
7.8183
7.8171
7.8067
7.6890
7.6865
7.6769
7.6745
5.4849
5.4828
5.4814
5.4793
5.1719
5.1706
5.1684
5.1673
2.3615
2.3600
2.3586
0.6007
Br
TMS
1.04
1.06
1.19
0.92
1.02
1.16
1.05
1.02
3.51
8.43
f1 (ppm)

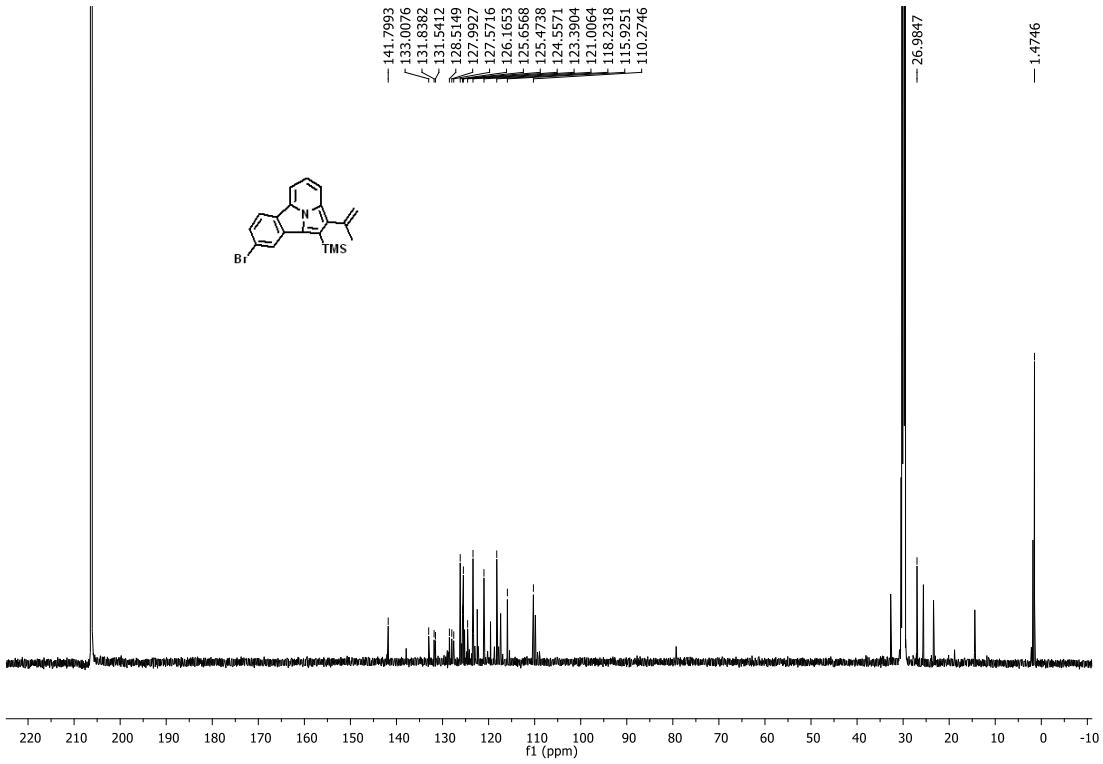
141.7993
133.0076
131.8382
131.5412
128.5149
127.9927
127.5716
126.1653
125.6568
125.4738
124.5571
123.3904
121.0064
118.2318
115.9251
110.2746
26.9847
1.4746
Br
TMS
f1 (ppm)

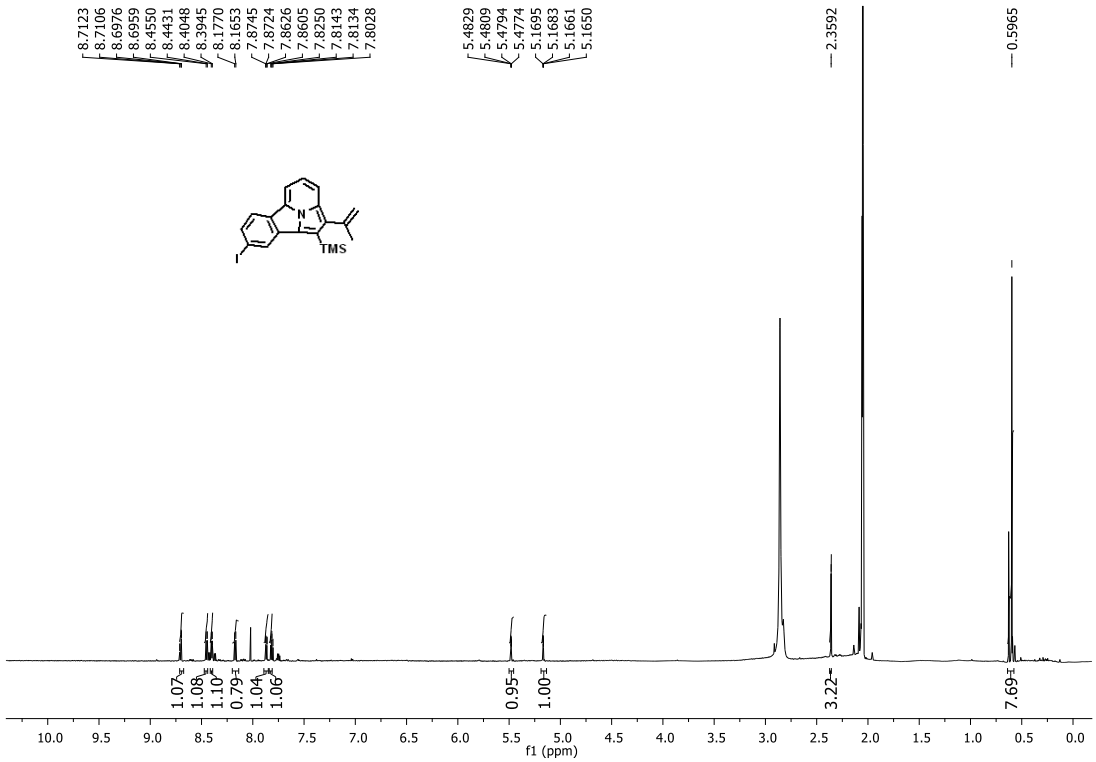
8.7123
8.7106
8.6976
8.6959
8.4550
8.4431
8.4048
8.3945
8.1770
8.1653
7.8745
7.8724
7.8626
7.8605
7.8250
7.8143
7.8134
7.8028
5.4829
5.4809
5.4794
5.4774
5.1695
5.1683
5.1661
5.1650
2.3592
0.5965
TMS
1.07
1.08
1.10
0.79
1.04
1.06
0.95
1.00
3.22
7.69
f1 (ppm)

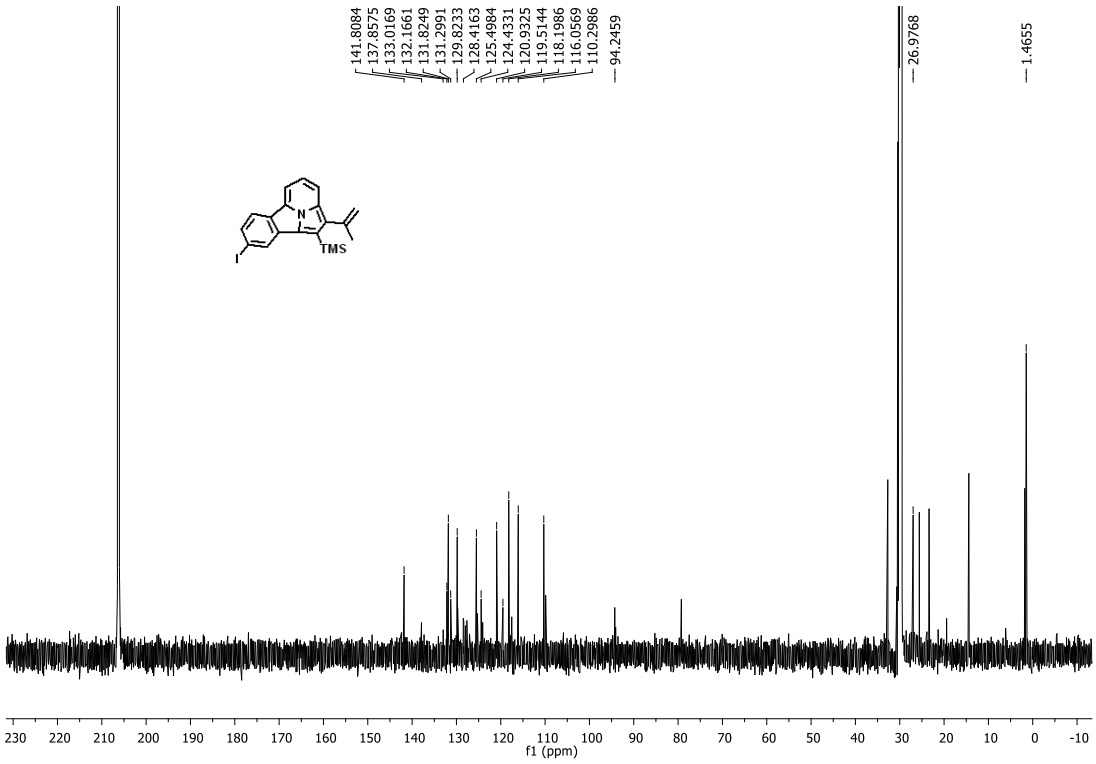
141.8084
137.8575
133.0169
132.1661
131.8249
131.2991
129.8233
128.4163
125.4984
124.4331
120.9325
119.5144
118.1986
116.0569
110.2986
94.2459
26.9768
1.4655
TMS
f1 (ppm)

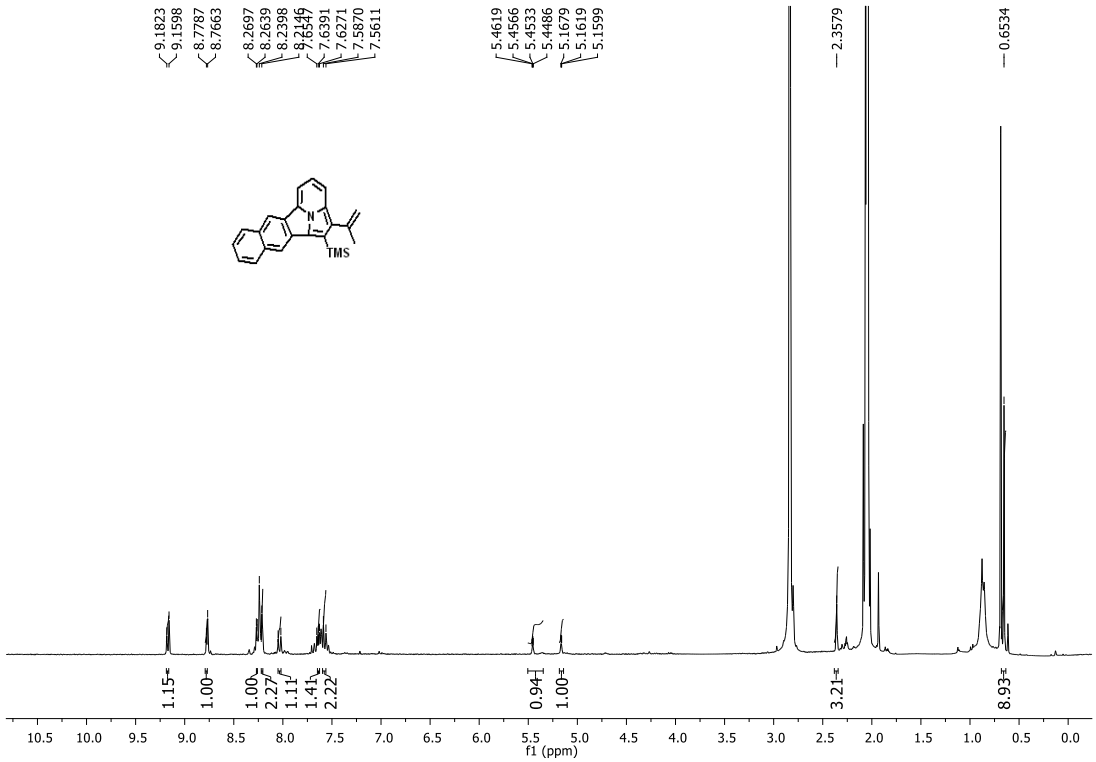
9.1823
9.1598
8.7787
8.7663
8.2697
8.2639
8.2398
8.2146
7.6547
7.6391
7.6271
7.5870
7.5611
5.4619
5.4566
5.4533
5.4486
5.1679
5.1619
5.1599
2.3579
0.6534
TMS
1.15
1.00
1.00
2.27
1.11
1.41
2.22
0.94
1.00
3.21
8.93
f1 (ppm)

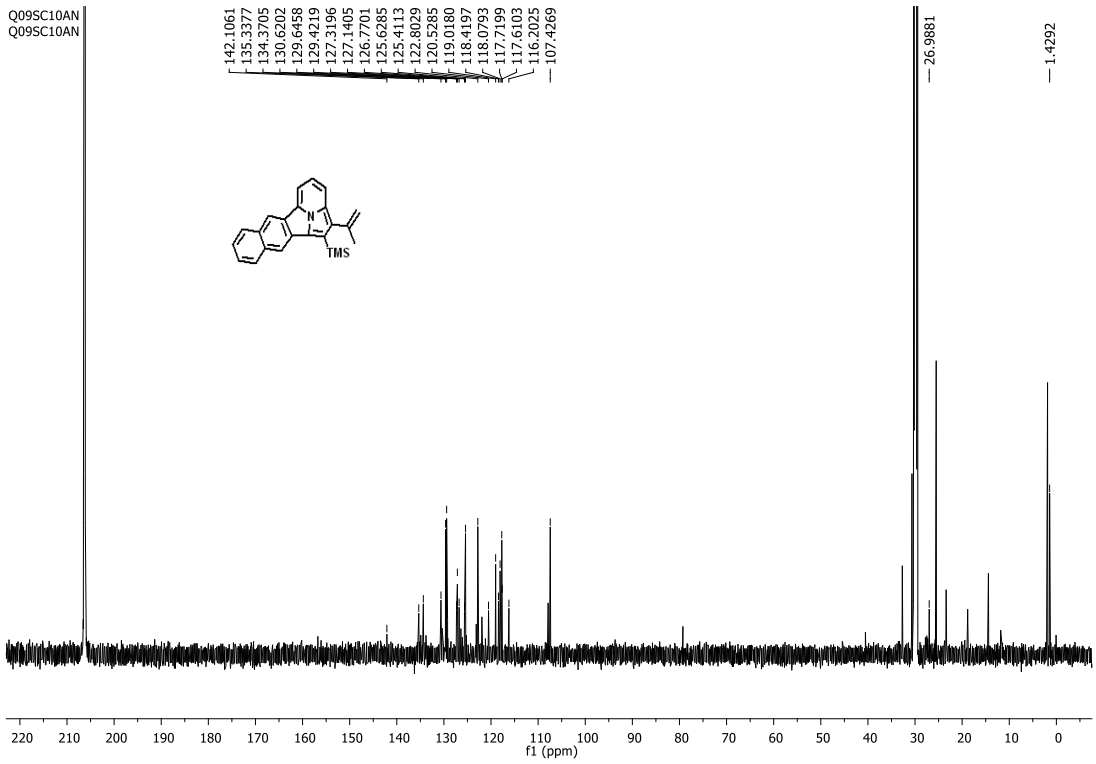
Q09SC10AN
Q09SC10AN
142.1061
135.3377
134.3705
130.6202
129.6458
129.4219
127.3196
127.1405
126.7701
125.6285
125.4113
122.8029
120.5285
119.0180
118.4197
118.0793
117.7199
117.6103
116.2025
107.4269
26.9881
1.4292
TMS
f1 (ppm)